



CIVIL ENGINEERING STUDIES

Smart Transportation Infrastructure Initiative Series No. xx-xxx [STII will provide]
UILU-ENG-20xx-xxxx [STII will provide]
ISSN: 0197-9191

Aerodynamic Survey of Novel eVTOL Configuration using SU2

Prepared By
Wanzheng Zheng
Jason M. Merret

University of Illinois at Urbana-Champaign

Research Report No. STII-xx-xxx [STII will provide]

A report of the findings of
eVTOL Configuration Understanding, Development, and Design

<https://doi.org/#####> (STII will provide)

Smart Transportation Infrastructure Initiative

March 2022

TECHNICAL REPORT DOCUMENTATION PAGE

1. Report No. STII will provide prior to posting	2. Government Accession No. N/A	3. Recipient's Catalog No. N/A
4. Title and Subtitle Aerodynamic Survey of Novel eVTOL Configuration using SU2		5. Report Date March/31/2022
		6. Performing Organization Code N/A
7. Author(s) Wanzheng Zheng Jason M. Merret		8. Performing Organization Report No. STII will provide prior to posting
9. Performing Organization Name and Address Smart Transportation Infrastructure Initiative Department of Civil and Environmental Engineering University of Illinois at Urbana-Champaign 205 North Mathews Avenue, MC-250 Urbana, IL 61801		10. Work Unit No. N/A
		11. Contract or Grant No. STII -21-XXX
12. Sponsoring Agency Name and Address		13. Type of Report and Period Covered STII will provide prior to posting
		14. Sponsoring Agency Code
15. Supplementary Notes https://doi.org/##### (STII will provide)		
16. Abstract The report summarized CFD results of eVTOL geometries using SU2 RANS solver. Geometries were generated based on STII Rappor 15 th iteration with different rotor installment solutions. It was found that although open rotors installed on an underwing pylon was superior than shrouded rotors installed in a canoe, the canoe configuration would see more potentials of improvements, and using a canoe door to cover the first rotor opening would reduce the drag received by canoe case below that of the rod case. Rotor doors were found to be the most efficient in reducing drag of the canoe case: Average drag reduction of covering the first rotor and all rotors were 66 counts and 165 counts, respectively. Changing rotor distributions along the chordwise direction have minimal impacts on drag reduction, and placing rotors along spanwise direction was not advised due to increase of projected frontal area. Increasing canoe chord length does not have significant impact on drag reduction, and if rotor doors were implemented, increasing canoe size has negative impact to drag. Rounding rotor edges does not change the aerodynamic performances of the canoe case, but will promote vertical air intake when running lifting fans. Drag received by the canoe parabolically correlated to rotor diameter, with 126 counts of drag if rotor diameter was 0 and 377 counts if rotor diameter was 2.95ft. Fuselage and tail added in average 179 counts of drag, and thus the aforementioned differences were still significant in the scale of aerodynamic properties of full configuration.		
17. Key Words Aerodynamics; Air taxi service; eVTOL CFD; Open rotors; Shrouded rotors; Urban air mobility; SU2	18. Distribution Statement No restrictions. This document is available through the National Technical Information Service, Springfield, VA 22161.	

19. Security Classif. (of this report) Enter security classification of this report (e.g. Unclassified). Reports carrying a security classification will require additional marking giving security and downgrading information as specified by the sponsoring agency.	20. Security Classif. (of this page) Enter the security classification of the form (e.g. Unclassified). When at all possible, Form DOT F 1700.7 should remain unclassified. If a classification is required, identify the classified items on the page by an appropriate symbol as per instruction from the sponsoring agency.	21. No. of Pages STII will add prior to posting	22. Price N/A
----------------------------------------------------------------------------------------------------------------------------------------------------------------------------------------------------------------------------------------------------------------------------------	------------------------------------------------------------------------------------------------------------------------------------------------------------------------------------------------------------------------------------------------------------------------------------------------------------------------------------------	-----------------------------------------------------------	-------------------------

Form DOT F 1700.7 (8-72)

Reproduction of completed page authorized

ACKNOWLEDGMENT, DISCLAIMER, MANUFACTURERS' NAMES

EXECUTIVE SUMMARY

Concept of vertical take-off vehicle, or informally, flying cars, was a long existing idea in the field of aviation. Recent advances in electrochemical power have generated a significant resurgence of interest in electric Vertical Take-off Landing Vehicle (eVTOL) aircraft [1]. An eVTOL was defined as a vertical lift aircraft propelled by electric power and capable of carrying people. Since the emergence of NASA Puffin eVTOL concept in 2009 [2], several industrial efforts were made, following which the concept was officially introduced by Vertical Flight Society and American Institute of Aeronautics and Astronautics in 2014 [3].

Foreseeable eVTOL civil applications ranged from delivery of passengers or packages to provision of emergency responses in a versatile manner. The novel vehicle concept could replace the role of conventional helicopters while offering the promise of safer, cleaner, quieter, and potentially cheaper operations. Companies, ranging from established aerospace corporations like Boeing and Airbus, to start-up companies like Lilium and Joby, were currently working on their own version of eVTOL, providing the market with various unique concepts of eVTOL designs [4].

With the choices available for the initial sizing of new vehicle designs, it was natural to question which type of configuration was most suitable. To provide a quantitative answer from an aerodynamic perspective to the problem posted above, two configurations were developed from STII geometry, one with open rotors installed on a rod under the wing and one with shrouded rotor installed in the wing was simulated and compared. Simulations were also performed to decide the sensitivity of other potential design variables.

It was observed that if no additional elements were added, rod with open rotor configuration was slightly superior than canoe with shrouded rotors. However, if rotor doors were taken into consideration, the canoe case had great potentials of improvements, receiving up to 26% less drag than the rod case. Covering the leading edge rotors provided the most drag reduction, and covering the first rotor along would provide a canoe configuration with better aerodynamic properties than the rod case. Lift and drag of the canoe case were relatively insensitive to design variables such as leading edge thickness, rotor distribution, and canoe chord length, providing freedom of modification with little change in aerodynamic properties.

Findings of this report suggested that a configuration with canoe and shrouded rotor installed within should be used if the vehicle was intended to cruise with fixed wing for better aerodynamic performances. This report also suggested that rotor openings should be covered as much as possible, starting from the leading edge rotors.

TABLE OF CONTENTS

TITLE OF REPORT GOES HERE	TITLE OF REPORT GOES HERE.....	错误!未定义书签。
ACKNOWLEDGMENT, DISCLAIMER, MANUFACTURERS' NAMES	I	
EXECUTIVE SUMMARY	II	
TABLE OF CONTENTS.....	III	
LIST OF FIGURES.....	IV	
LIST OF TABLES	VI	
CHAPTER 1: INTRODUCTION	1	
CHAPTER 2: METHODS AND VERIFICATIONS.....	2	
Geometry and CFD Methods	2	
Convergence and Validation Study.....	6	
CHAPTER 3: ROD AND CANOE CONFIGURATION.....	9	
CHAPTER 4: VARIATION SENSITIVITY OF CANOE CASE	11	
Effect of Canoe Thickness	11	
Effect of Canoe Doors	12	
Effect of Rotor Placements	18	
Effect of Leading Edge Modifications	22	
Effect of Rounding Rotor Edges	26	
Effect of Rotor Diameters	28	
CHAPTER 5: FULL CONFIURATION SURVEY	30	
CHAPTER 6: CONCLUSION AND FUTURE WORK	32	
REFERENCES.....	34	

LIST OF FIGURES

Figure 1 Photos of eVTOL Designs of Different Categories	2
Figure 2 CAD Model of the Rod Case.....	3
Figure 3 CAD Model of the Canoe Case.....	4
Figure 4 Y+ Value of Baseline Cases.....	5
Figure 5 Surface Mesh of Convergence Study.....	7
Figure 6 Convergence of Drag Coefficient for the Test Case.....	7
Figure 7 Test Case for Validation Study.....	8
Figure 8 Comparison Between Predictions of Different CFD Methods.....	8
Figure 9 Aerodynamic Differences with Rotor Addition	9
Figure 10 CAD Model of Canoe, Rod (Single and Double Column) with Wing	10
Figure 11 Aerodynamic Properties of Canoe, Rod (Single and Double Column) with Wing.....	11
Figure 12 CAD of Canoe Case with Varying Canoe Thickness	13
Figure 13 Aerodynamic Properties of Canoe Case with Varying Canoe Thickness	13
Figure 14 CAD Model of Canoe Case with Rotor Naming	14
Figure 15 Aerodynamic Properties of Canoe Case Covering First and Second Rotor Openings.....	14
Figure 16 Aerodynamic Properties of Canoe Case Covering Individual Rotor Openings.....	15
Figure 17 Aerodynamic Properties of Canoe Case Covering Consecutive Rotor Openings	16
Figure 18 CAD Model of Canoe Case Integrated with Wing.....	17
Figure 19 Aerodynamic Properties of Canoe Cases with Wing	17
Figure 20 CAD of Canoe Case with Different Rotor Placement Methods	19
Figure 21 Aerodynamic Properties of Canoe Case with Different Rotor Placements.....	19
Figure 22 Visualization of Cf Distribution of Canoe Case with Different Rotor Placements.....	20
Figure 23 CAD of Canoe Case with Different Rotor Chordwise Distribution.....	20
Figure 24 Aerodynamic Properties of Canoe Case with Different Rotor Chordwise Distribution	21
Figure 25 Pressure Comparison of Canoe Section with Different Rotor Chordwise Distribution.....	21
Figure 26 CAD of Canoe Case with Varying Canoe Chord Length	22
Figure 27 Aerodynamic Properties of Canoe Case with Varying Canoe Chord Length.....	23
Figure 28 L/D of Canoe Case with Varying Canoe Chord Length at 8 Degree Angle of Attack	24

Figure 29 CAD of Canoe Case with Varying Canoe Chord Length with Rotor 1 Covered.....	24
Figure 30 Aerodynamic Properties of Canoe Case with Varying Chord Length, Rotor 1 Covered.....	26
Figure 31 Cp distribution of Canoe Case with Rounded Rotor Edge.....	27
Figure 32 Pressure Comparison of Canoe Section with Rounded Rotor Edge	27
Figure 33 Aerodynamic Properties of Canoe Case with Rounded Rotor Edge.....	28
Figure 34 CAD of Canoe Case with Different Rotor Diameter.....	29
Figure 35 Aerodynamic Properties of Canoe Case with Different Rotor Diameter	29
Figure 36 L/D Contour of Canoe Case with Different Rotor Diameter.....	30
Figure 37 CAD of Canoe and Rod Cases with Fuselage and Tail.....	31
Figure 38 Aerodynamic Properties of Full Configurations	31
Figure 39 Cp Distribution of Full Configuration.....	32
Figure 40 CAD of Possible New Configuration.....	35

LIST OF TABLES

Table 1 Simulation Environments.....	5
Table 2 Drag Reduction of Covering Consecutive Rotor Openings	15
Table 3 Average Drag Difference for Different Rotor Chordwise Distribution	20
Table 4 Average Drag Difference for Varying Canoe Chord Length	25
Table 5 Summary of Trade Elements and Respective Drag Differences	32

CHAPTER 1: INTRODUCTION

Electronic Vertical Take-off and Landing (eVTOL) aircraft has generated significant interest thanks to their versatile application, and recent advances in electrochemical [1] [3]. The novel vehicle concept could replace the role of conventional helicopters while offering the promise of safer, cleaner, quieter, and potentially cheaper operations. Companies, ranging from established aerospace corporations like Boeing and Airbus, to start-up companies like Lilium and Joby, were currently working on their own version of eVTOL, providing the market with various unique concepts of eVTOL designs [4]. Generally, classification of eVTOL could be made on their operation mechanism and configuration. A few current configurations that were representative to their respective design philosophy were listed in Figure 1 [5][6][7][8][9]. Designs depended on rotors to provide lift and thrust included electric helicopter and multi-copters, and designs that required wings to provide lift during cruise included tilt-rotor design, fixed wing with vector thrust design, and lift and cruise hybrid design [10]. Initial sizing study suggested that all-rotor configurations required higher energy demands and thus only feasible for shorter ranges [11]. For the interest of this project, lift and cruise hybrid design was chosen as baseline due to the high range requirement for air taxi.

Current winged eVTOL configurations seen in the market often feature open rotors installed in underwing pylons (rod) to achieve vertical take-off and landing. While such configurations were the most intuitive and perhaps easiest to accomplish from an integrated standpoint, with the development of the eVTOL industry, novel designs using shrouded rotors were also becoming popular. With the choices available for the initial sizing of new vehicle designs, it was natural to question which type of configuration was most suitable for the intended mission profile. To provide a quantitative answer from an aerodynamic perspective to the problem posted above, two configurations were developed from STII geometry, one with open rotors installed on a rod under the wing and one with shrouded rotor installed in the wing (canoe) was simulated and compared. Simulations were also performed to decide the sensitivity of other potential design variables, namely rotor sizing and spacing, canoe thickness, and rotor doors.

This report provides simulation results of the aforementioned configurations, as well as other variations derived from the baseline geometry using SU2 CFD packages. Basic explanations of geometries and simulation methods were explained in Chapter 2. Comparison between different means of installing rotors was made in Chapter 3. Derivative geometries by varying design parameters were made in Chapter 4 to determine the driving factors of aerodynamic performance on shrouded rotor configuration. A batch of simulations on various wing designs on fuselage was made in Chapter 5 to determine the significance of the discussions in previous chapters. Finally, conclusions were drawn from presented data in Chapter 6 to offer qualitative to semi-quantitative suggestions in future iterations of this eVTOL vehicle.



Figure 1 Photos of eVTOL Designs of Different Categories

Source: Tier 1 Engineering; Volocopter; Pipistrel; Joby Aviation; Lilium Air Mobility

CHAPTER 2: METHODS AND VERIFICATIONS

GEOMETRY AND CFD METHODS

The current configuration of interest was built upon the 15th iteration of the STII Rappor design. The first 14 iterations varied in wing, and other basic factors of vehicle sizing and resulted in with a semi-definite design on which forms the basis of this study. A schematic of the full-scale geometry was shown in Figure 2 and Figure 3, in which the main interest of this study focused on the wing and rotor placements. The canoe consists of a NACA 0006 airfoil with a span of 20 ft and a width of 4ft. The rod has a diameter of 1ft and was rounded at the two ends with hemispheres, and each hub has a diameter of 10 in and a height of 11 in. Rotors are placed symmetrically with respect to the center chord and the rotor size was chosen to be 1.96 ft and was held constant unless it was a variable of interest. Two major configurations of interest were the shrouded rotor installed on a canoe, from here on the canoe case, and the open rotors installed under the wing, from here on the rod case. Since the rod case does not require an extended wing section to install shrouded rotors, the canoe was removed in the rod case with the root airfoil and the wing airfoil held at constant shape and positions.

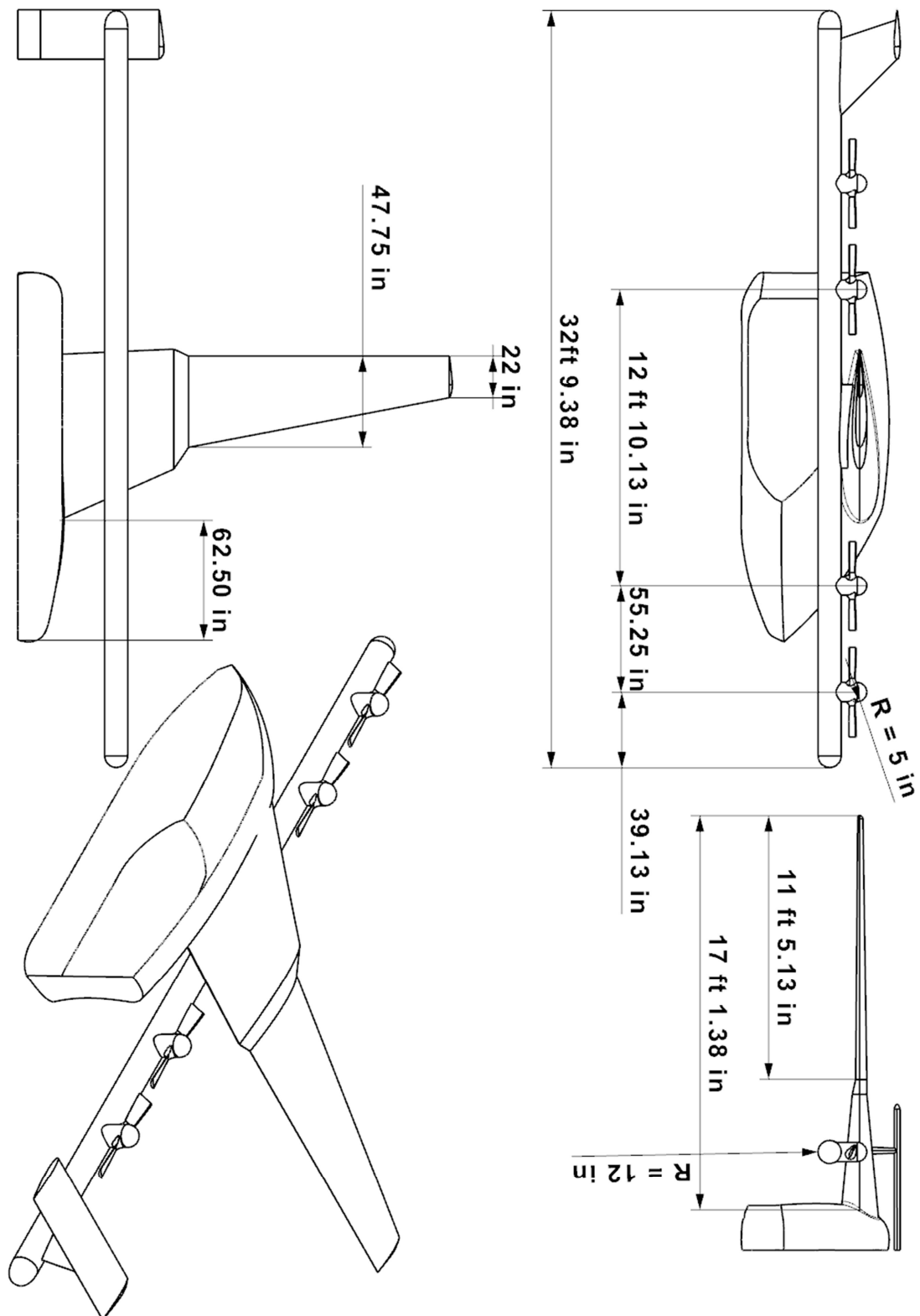


Figure 2 CAD Model of the Rod Case

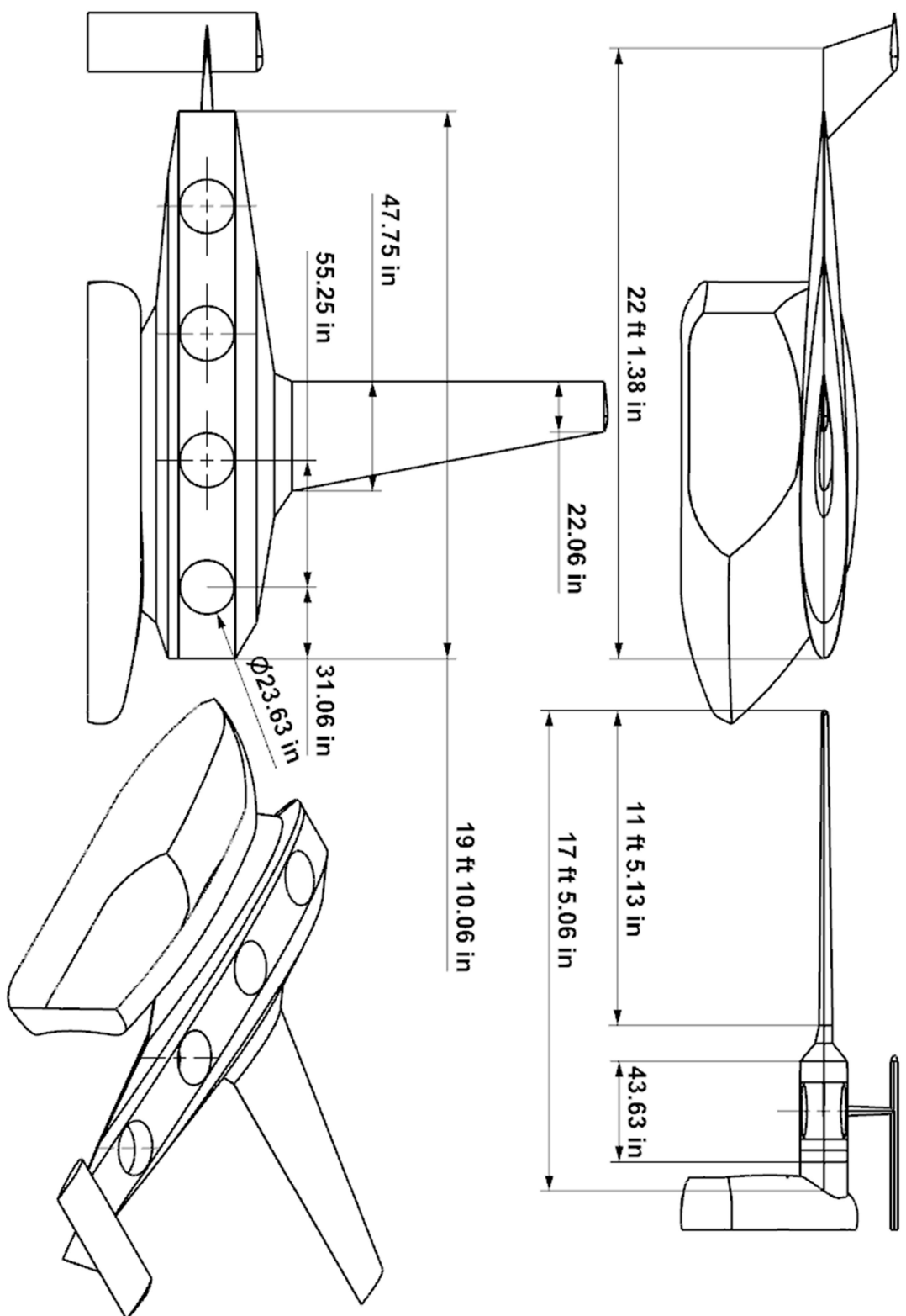


Figure 3 CAD Model of the Canoe Case

Aerodynamic performances was collected using SU2 CFD Reynold Number Averaged Navier Stokes (RANS) solver [12] with flight condition set for 0.1 Mach at sea-level standard atmosphere at angles of attack ranging from 0 to 8 degrees with 2-degree intervals. Variables of interest for this CFD simulation were listed in Table 1. The meshing of geometries was performed in Pointwise [13] using hybrid cells. The average cell size was chosen to be 0.01 to balance computational expenses and simulation accuracy. Details of the convergence study were presented in the following sub-chapter. Cell height on the first later was estimated to be 1.2E-5 with a normal growth rate of 1.2 to achieve a $y+$ value less or equal to 1. A surface $y+$ contour was presented in Figure 4. Surface $y+$ values were only examined for baseline cases shown in Figure 2 and Figure 3, as the RANS solver could resolve high boundary layer cells using wall functions. A semispherical domain was created and labeled as pressure far-field with respective Mach number and total pressure of the standard sea-level atmosphere. Convergence criteria was set that root mean square error of drag coefficient to be less than 1E-6. Results shown in this report has all satisfied such convergence criterion.

Table 1 Simulation Environments

Variables	Metric Units	Imperial Units
Reynolds Number	12.3E+06	12.3E+06
Mach Number	0.1	0.1
Velocity	34.030 [m/s]	111.6 [ft/s]
Temperature	288.15 [K]	518.7 [R]
Characteristics Length	6 [m]	19.7 [ft]
Reference Area	15.236 [m^2]	163.9 [sqft]

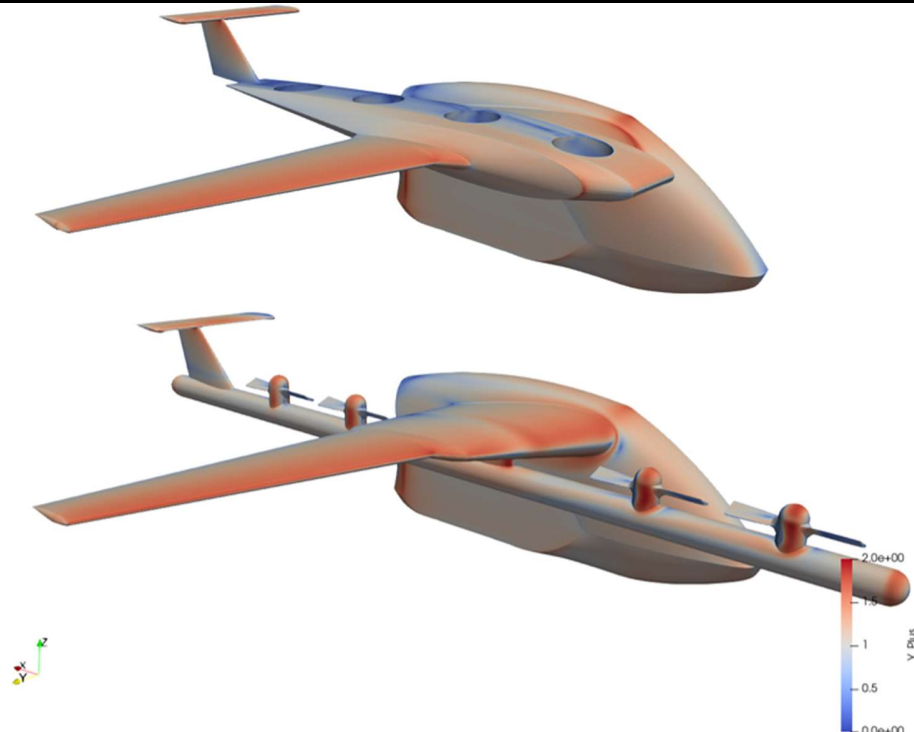


Figure 4 $Y+$ Value of Baseline Cases

CONVERGENCE AND VALIDATION STUDY

This study intended to ensure the quality of results. The problem was divided into three aspects and was investigated separately. It was well known that the solver chosen for this study was dependent on cell quality and resolution of the mesh. A set of simulations was conducted to ensure adequate grid quality was applied by running a convergence study on meshes with the same geometry and simulation conditions but different cell densities. Cell density was measured by average edge length between nodes on the surface mesh (Δs). Δs chosen for the convergence study ranged from overly coarse (0.02) to very fine (0.004), and convergence of aerodynamic parameter should be observed in between, indicating an adequate mesh density that offers reliable results while remaining computationally efficient. A further validation study was conducted to ensure consistency of results by comparing simulation results from two different CFD methods. Finally, a comparison was done between RANS solver and Euler's solver corrected by empirical methods to ensure the chosen turbulence model was correct.

The convergence study test case consists of the wing part of the configurations of interests, shown in Figure 5. Mesh consists of fully structured mesh on the wing and unstructured mesh at the wing cap at tip of the wing. A further analysis was performed on the canoe case to ensure that convergence behavior was identical to that of the test case. The results of the convergence study were shown in Figure 6. A set of simulations was then conducted on just the canoe that were more geometrically complex compared to the test case. Convergence trend of this simulation matched that observed in the convergence study. It was thus determined that an average cell size of 0.01 would suffice for the scope of this study as its value deviates less than 3% from the converged value.

A simulation was conducted and results were compared with that predicted by a different CFD package: STAR CCM+. Configuration of interest consists of the canoe with no wing attached with various rotor openings covered, shown in Figure 7. The verification used RANS solver from SU2 comparing to constant density equation of state with SST K- ω turbulence model from STAR-CCM+. All initial conditions are set to that shown in Table 1. A comparison of the results was shown in Figure 8. RANS solver in SU2 tends to over predict drag compared to that predicted by STAR CCM+, but overall, the comparison showed significant similarity between the results obtained from the two methods. Most importantly the relative difference and the trend of aerodynamic coefficient to angles of attack were identical. This comparison and the display of encouraging similarity offered more confidence in the physical correctness of SU2 predictions used later in this report. Another comparison was made for the rod case between RANS solver and Euler solver corrected by empirical methods. The two solvers of interest provided identical results in drag prediction, inferring that the turbulence model of choice is accurate for the scope of this study.

It should be noted that separated flow was not represented correctly with the choice of solver and turbulence model. However, the results presented was still valid for comparison purposes, which was the major interest of this study.

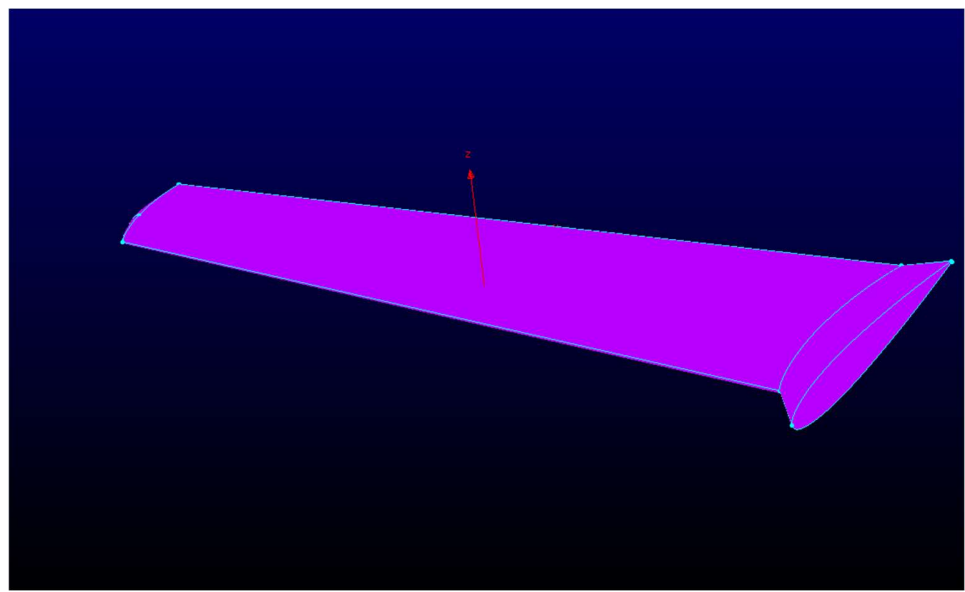


Figure 5 Surface Mesh of Convergence Study

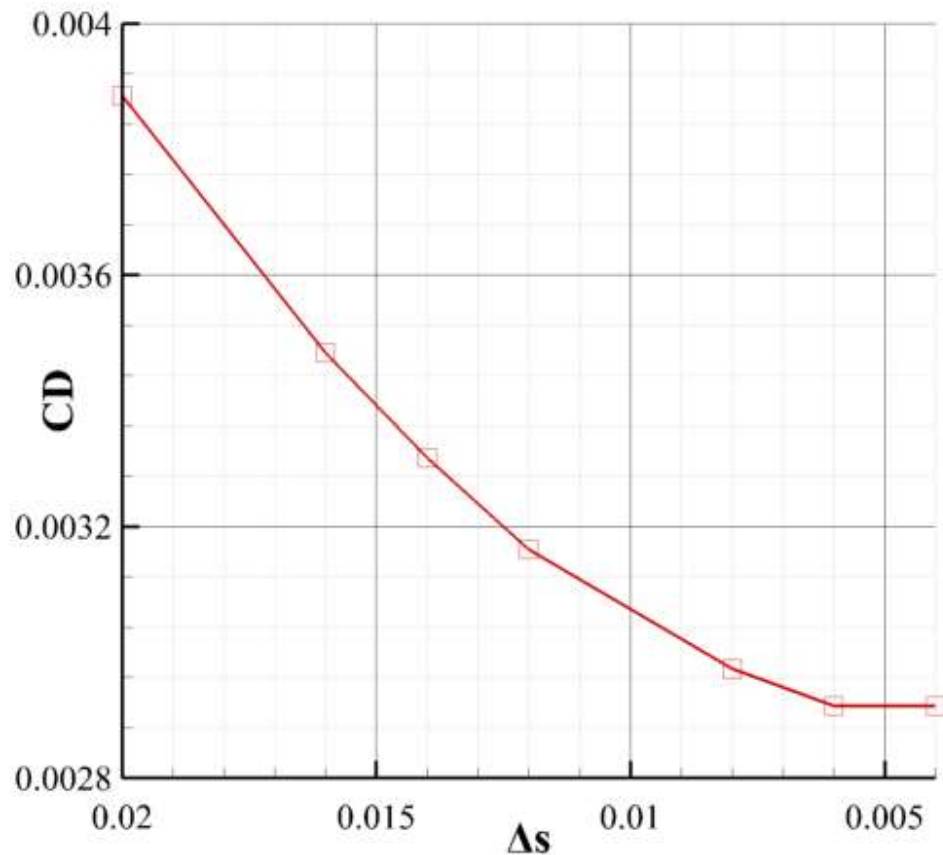


Figure 6 Convergence of Drag Coefficient for the Test Case

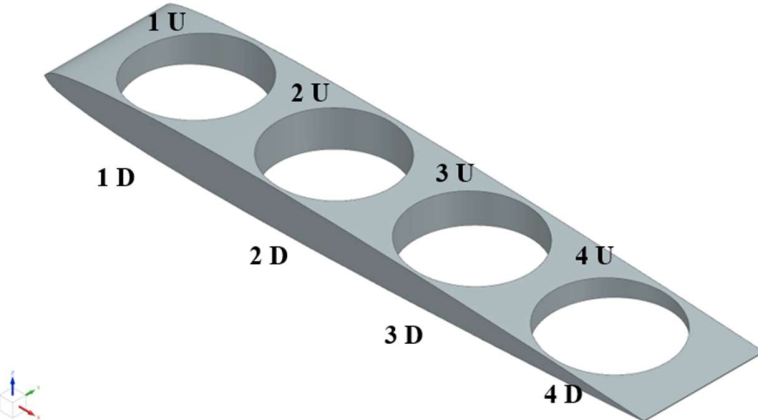


Figure 7 Test Case for Validation Study

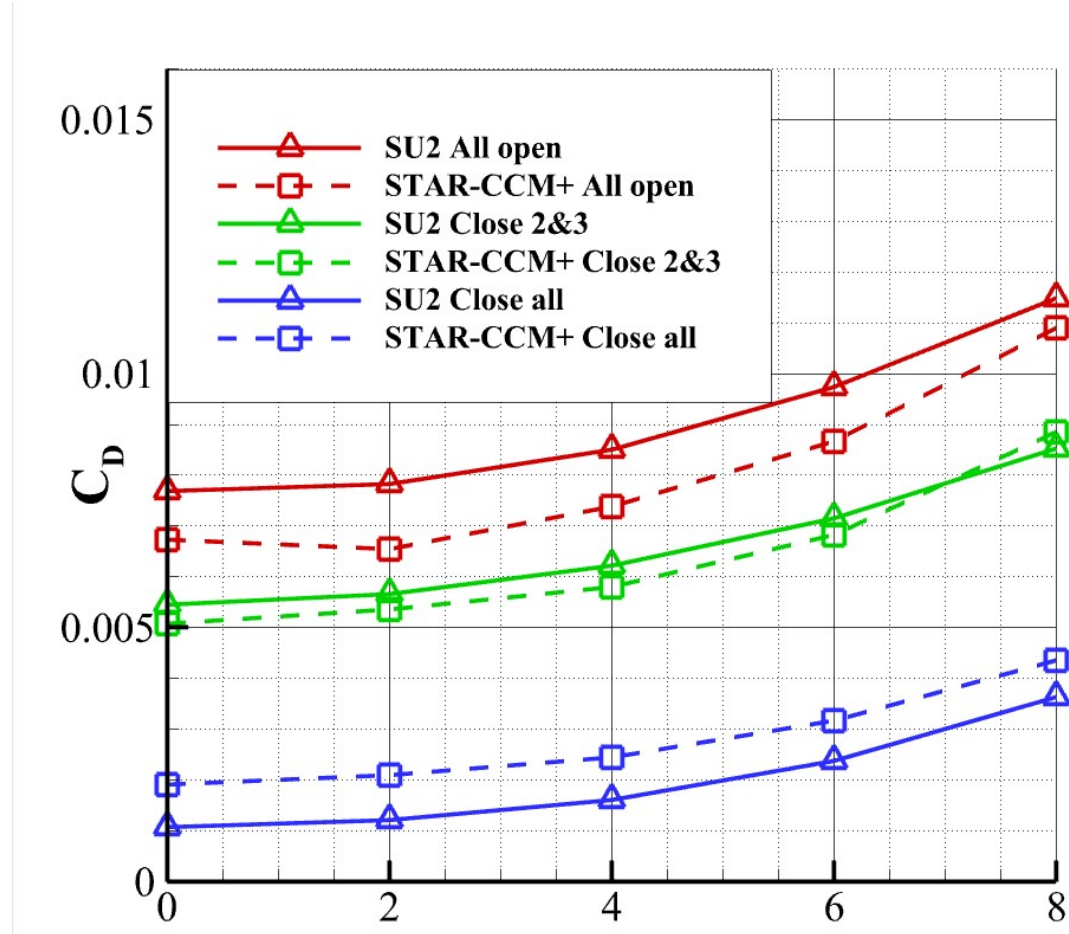


Figure 8 Comparison Between Predictions of Different CFD Methods

CHAPTER 3: ROD AND CANOE CONFIGURATION

This report first discussed the effect of including rotor blades on aerodynamic properties. Simulations were performed on individual configurations with and without rotor blades installed. The results were presented in Figure 9. The three polars, starting from top left to bottom, were drag polar, lift coefficients versus angles of attack, and lift over drag versus angles of attack. It was observed that adding rotors will improve aerodynamic properties for the canoe case while slightly worsening that of the rod case. Maximum differences on drag coefficient were around 20 counts compared to respective configurations without rotors. Adding rotors partially prevented recirculation in open shrouds for the canoe case while provoking larger flow separation on the rod case, which explained why adding the same component may negatively impact drag characteristics for one configuration while positively impacting the other. For simplicity purposes, the effect of rotors was not considered for further simulations consisting of comparative features of the canoe. Note the decrease of L/D of rod case at 2-degree angle of attack was also observed in simulations conducted using STAR-CCM+. The reason of such phenomenon was not yet investigated as it was not among the major interest of this study.

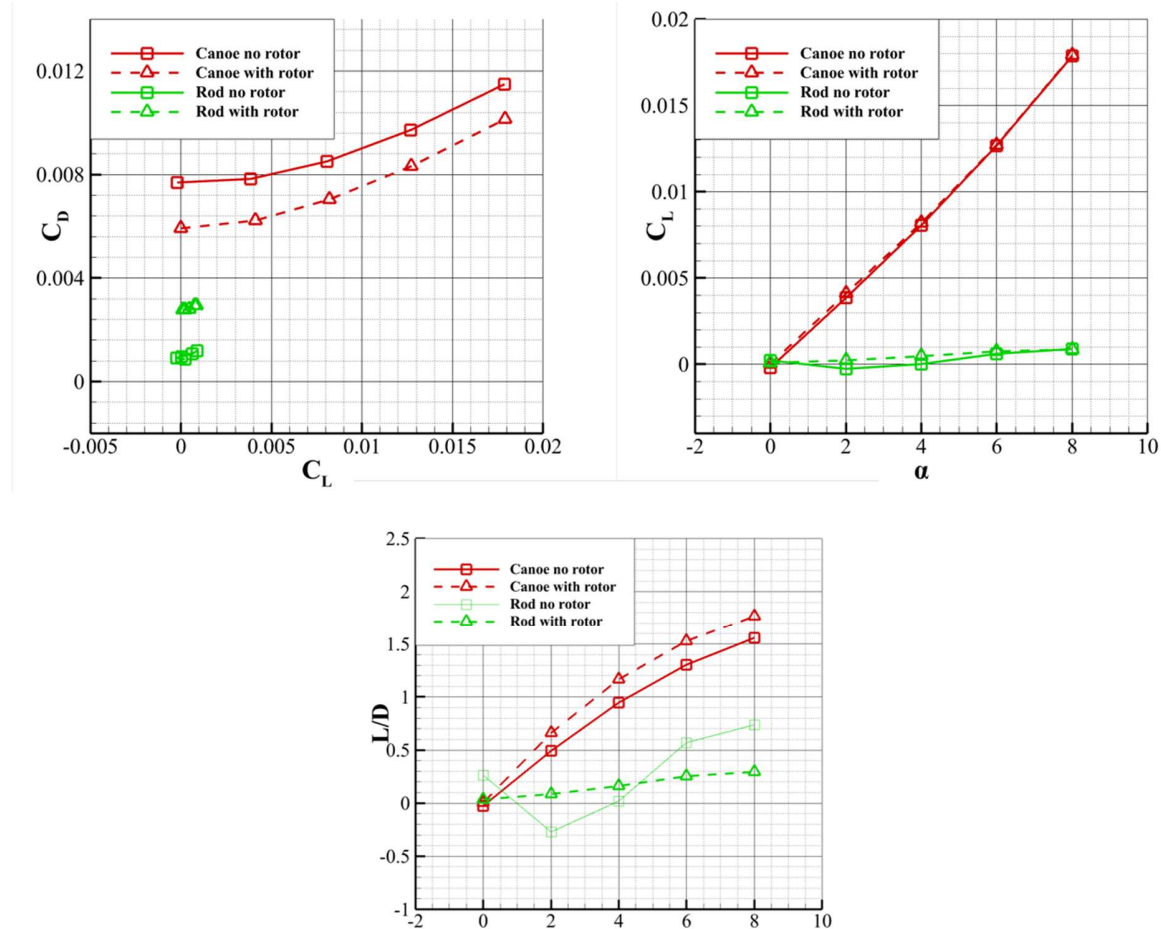


Figure 9 Aerodynamic Differences with Rotor Addition

The rod and canoe configurations were then integrated with the wing design of the 15th iteration, shown in Figure 10. A new configuration was added in which the rod was split into two and installed separately underwing. Aerodynamic properties of the two configurations were compared in Figure 11.

The four polars, starting from top left to right bottom, were drag polar, lift coefficients versus angles of attack, lift over drag versus angles of attack, and induced drag over lift versus lift coefficients. The first plot quantitatively illustrated drag characteristics at various flight conditions, the second plot illustrated the sensitivity of lift with respect to vehicle orientation, and the last two plot illustrated lift over drag, which is related to vehicles range and endurance capability, and the efficiency factor that related drag to lift squared. Such four plots would be presented for further simulations to offer in-depth visualization of results and their inferences.

It was observed that the canoe harbors similar aerodynamic characteristics of the rod at low angles of attack but quickly diverged as angles of attack increased and larger flow separation began to occur. However, the canoe case has more possibilities in integrating elements such as canoe doors which potentially would improve its aerodynamic performances. Further studies were conducted to quantitatively specify such potentials in the following sections. From an aerodynamics perspective, it was not advised to use multiple underwing pylons for the increase in the frontal area will cause drag increase.

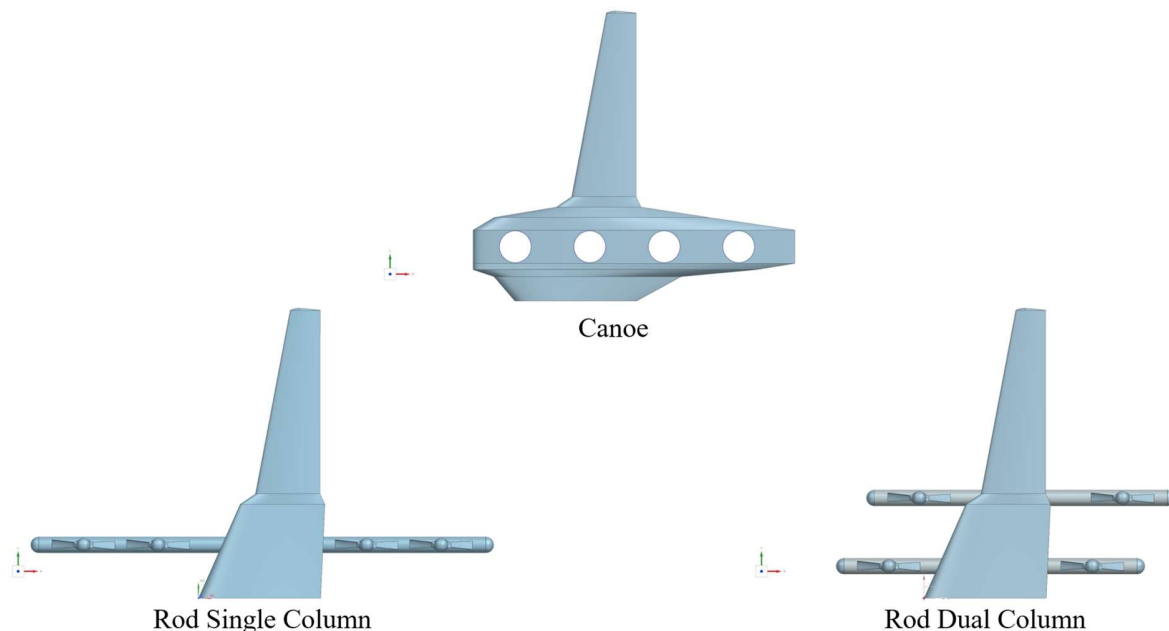


Figure 10 CAD Model of Canoe, Rod (Single and Double Column) with Wing

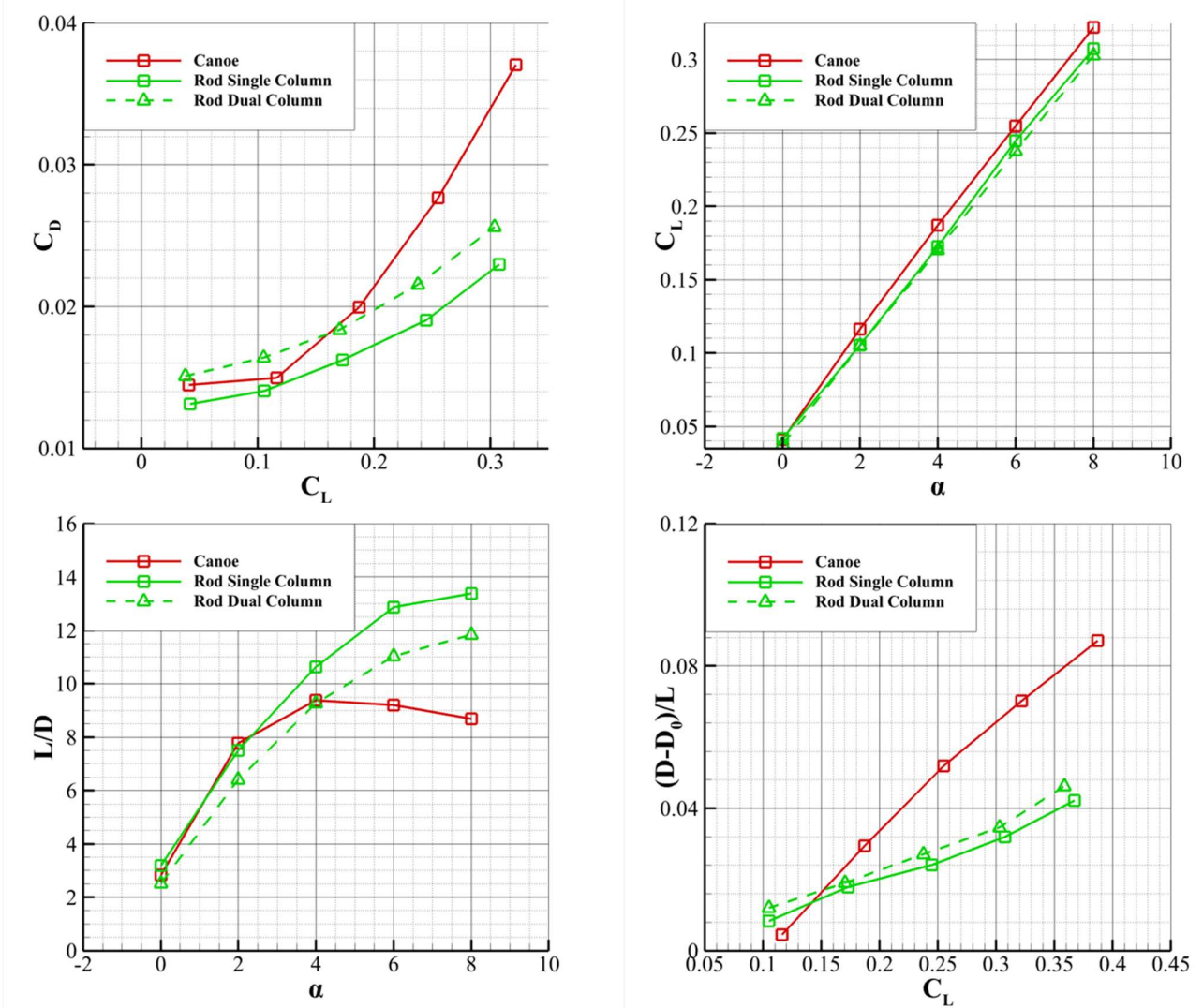


Figure 11 Aerodynamic Properties of Canoe, Rod (Single and Double Column) with Wing

CHAPTER 4: VARIATION SENSITIVITY OF CANOE CASE

Implementing these modifications would inevitably introduce more weight to the current design and cause new aeroelastic concerns, which changed the nature of the problem of interest into a multi-objective multi-disciplinary optimization (MDO). While the above optimization problem was not performed in this report, it would certainly be a function of the sensitivity of aerodynamic properties with respect to each potential design variable, either single or coupled. Therefore, this section aims to provide quantitative information on how each possible modification to the baseline case will impact the overall aerodynamic performance of the canoe case. In the future, the aforementioned MDO problem could be formulated and performed with additional considerations such as weight, structural and intended mission profile of the vehicle.

EFFECT OF CANOE THICKNESS

As the stagnation in rotor openings was acknowledged as a major source of drag, an investigation of varying canoe thickness was carried out. A thinner canoe would potentially decrease the frontal area of the vehicle. Two configurations of interest were modified based on the canoe configuration, all rotors covered or all rotors open, with canoe thickness decreased by 25%. The models of interest were shown in Figure 12, and the simulation results were shown in Figure 13. Varying canoe thickness does not significantly interfere with drag characteristics, as the modification resulted in, on average, less than 10 counts of drag difference from their baseline cases, respectively. This was likely due to the thickness of the canoe being already thin, compared to the chord length, as NACA 0006 was chosen to be the canoe airfoil.

EFFECT OF CANOE DOORS

Canoe doors could be added to prevent early separation caused by the shrouded rotors installed. A set of simulations was conducted to investigate whether covering the upper, the lower, or both of the shrouded rotor was necessary. A schematic of the Canoe configuration with naming conventions was presented in Figure 14. Each rotor hole was covered individually on the suction, pressure, or both sides, namely X_U , X_D , and $X_{U/D}$, where X is the rotor number. The result polar of these cases were shown in Figure 15. Adding a canoe door improved the aerodynamic properties of the configuration and covering the pressure, or lower, surface was slightly more efficient than covering the suction, or upper, surface. However, such difference was trivial compared to the drag reduction by covering both holes of the rotor, and thus the option of closing only one surface of a rotor was not taken into consideration further on. For simplicity in nomenclature, closing both upper and lower surfaces of any rotor openings was represented by the number of the respective openings alone, and the previous subscripts of U/D were dropped.

It was also observed that covering the first rotor along the leading edge offered more drag reduction than covering the second rotor since the pressure side experienced larger pressure differences. A survey was conducted to further solidify this intuition by covering each rotor hole, shown in Figure 16. Drag reduction decreases as the rotor covered shifts from the leading edge to the trailing edge, and the maximum difference between these configurations of interests, namely cover 4 and cover 1, was 16 counts on average. Thus, it was concluded that consecutive rotor openings, starting from the leading edge, should be covered to yield optimal drag reduction.

A wholistic survey was conducted in investigating effect of positions which rotor openings were covered was conducted. From previous results, only modifications of consecutive openings on both suction and pressure sides were considered. The polar of this survey was shown in Figure 17. Average reduction in drag with respect to the all-open case was concluded in Table 2.

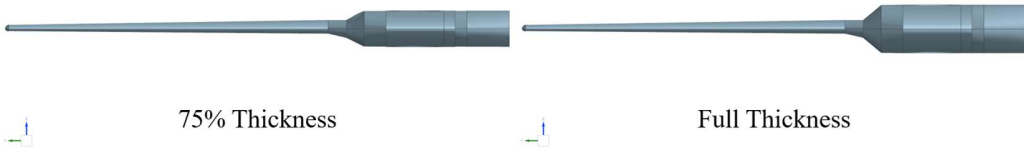


Figure 12 CAD of Canoe Case with Varying Canoe Thickness

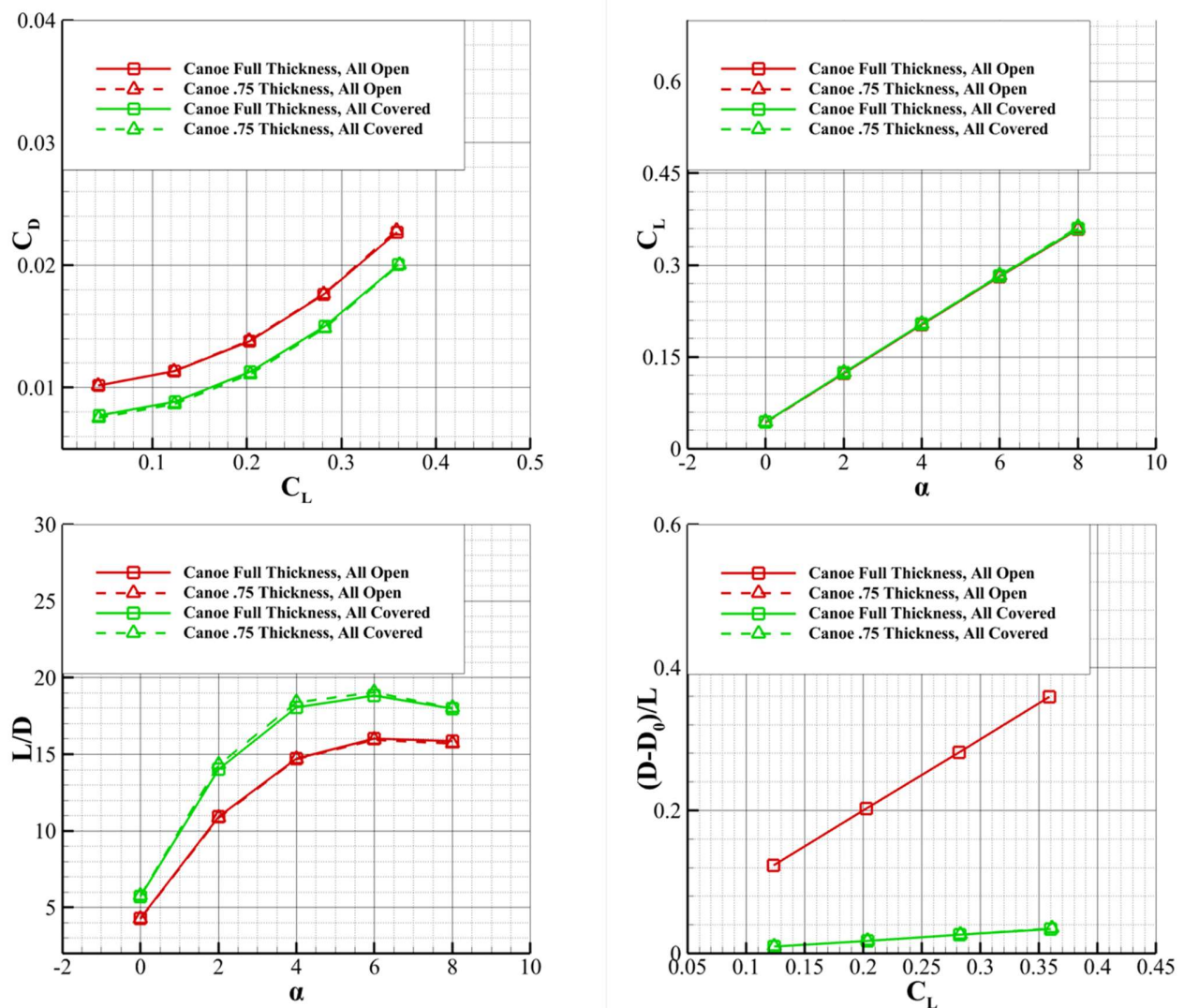


Figure 13 Aerodynamic Properties of Canoe Case with Varying Canoe Thickness

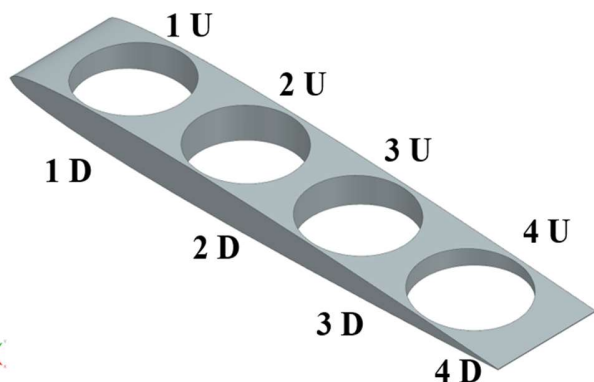


Figure 14 CAD Model of Canoe Case with Rotor Naming

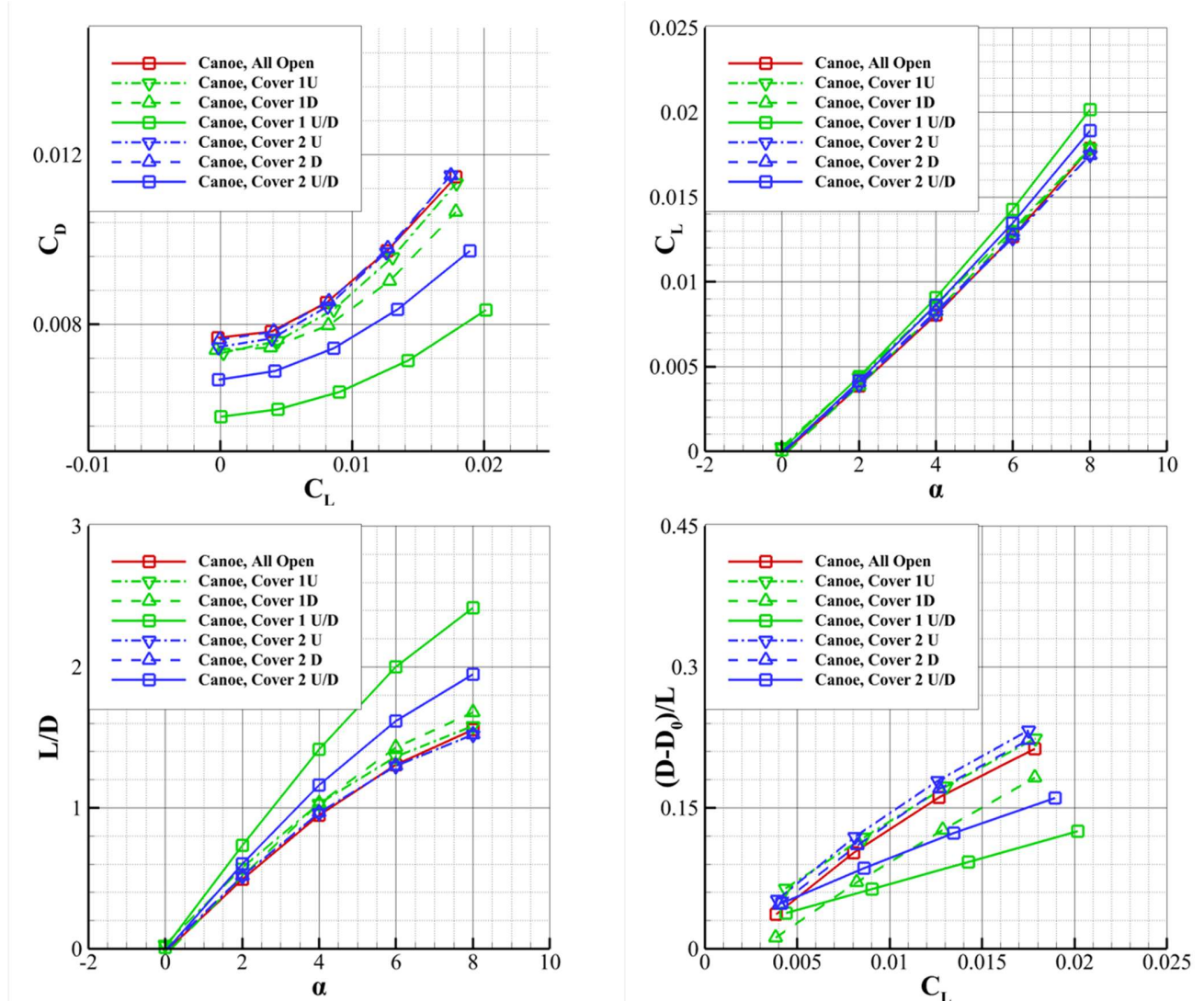


Figure 15 Aerodynamic Properties of Canoe Case Covering First and Second Rotor Openings

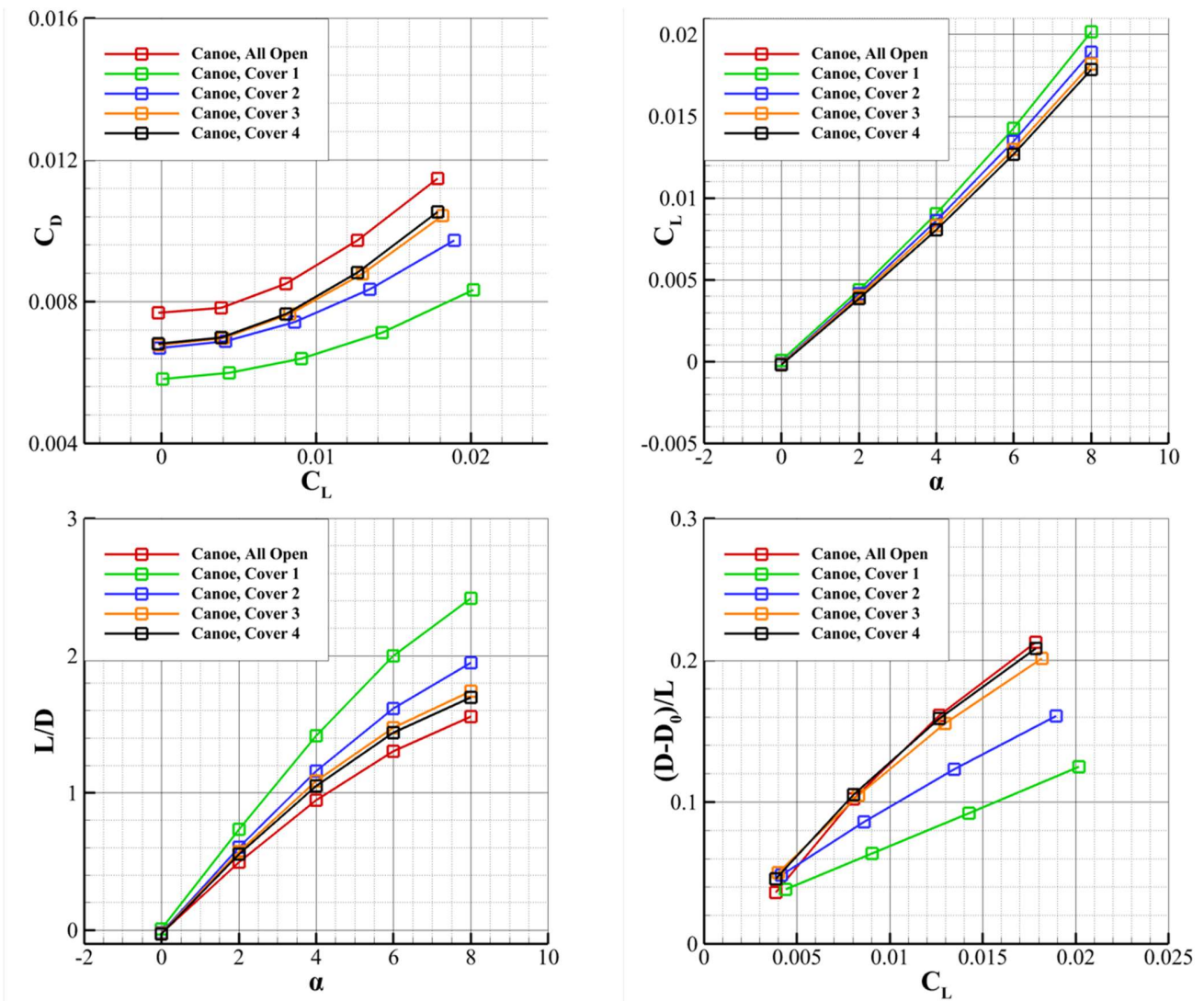


Figure 16 Aerodynamic Properties of Canoe Case Covering Individual Rotor Openings

Table 2 Drag Reduction of Covering Consecutive Rotor Openings

Configuration	Average Drag Reduction (counts)	Average Percent of Reduction
Close 1	23.1	25.5%
Close 1 & 2	36.3	40.1%
Close 1, 2, & 3	52.0	57.5%
Close 1, 2, 3, & 4	70.6	78.1%

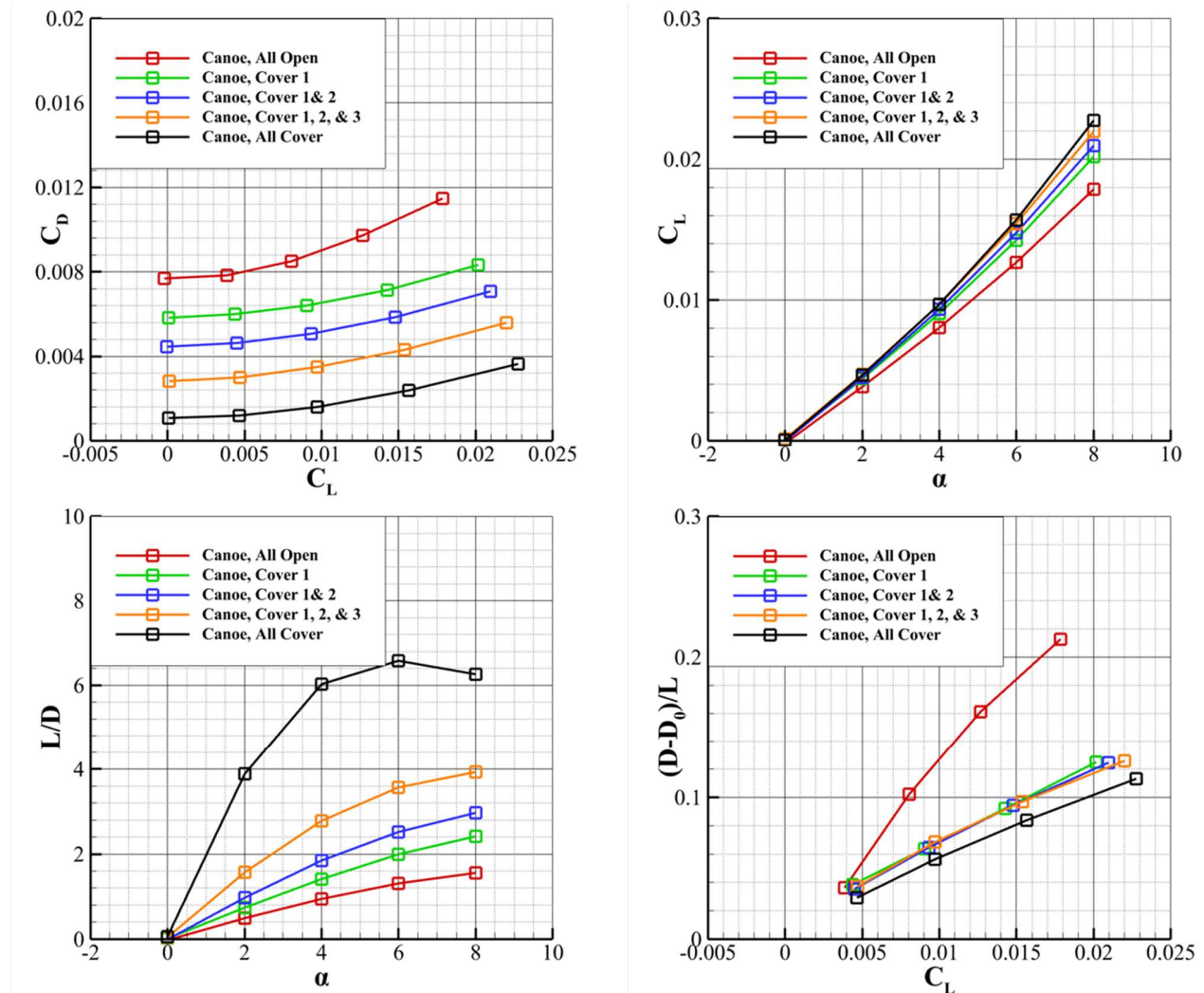


Figure 17 Aerodynamic Properties of Canoe Case Covering Consecutive Rotor Openings

Finally, the same simulation was carried out for canoe cases integrated with the wing to ensure that drag reduction observed above was still significant on a more representative scale of geometry. The rotor naming convention followed that presented in Figure 14 and was shown again in Figure 18 with the current configuration of interest. The result of the simulation was shown in Figure 19. Quantitatively, covering rotor number 1, number 1 and 2, number 1, 2, and 3 would yield drag reduction of 22%, 33%, and 38%, respectively, compared to the all-open case. This result offered quantitative insight in adding canoe doors to the current configurations, as additional elements introduce more weight into consideration, and adding canoe doors to certain rotor openings was more cost-effective. For comparison purposes, simulation result of rod cases with wings attached were also shown in Figure 20. It was observed that with the first rotor door added, canoe case would perform similarly as single rod case, therefore further solidifying the conclusion that canoe configuration has more potential in drag reduction than the rod cases.

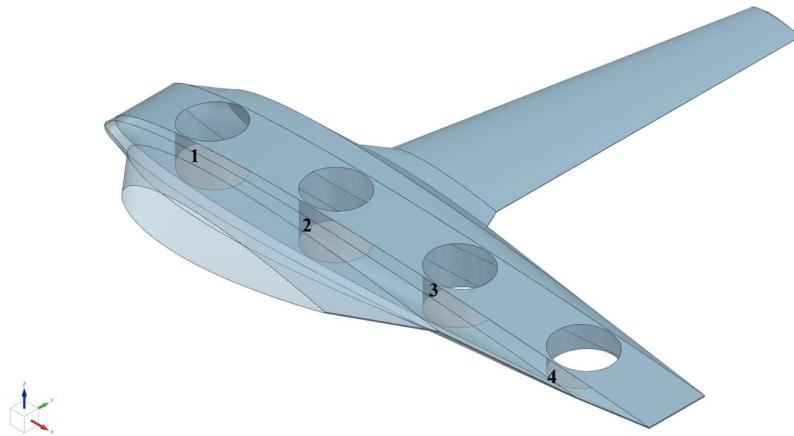


Figure 18 CAD Model of Canoe Case Integrated with Wing

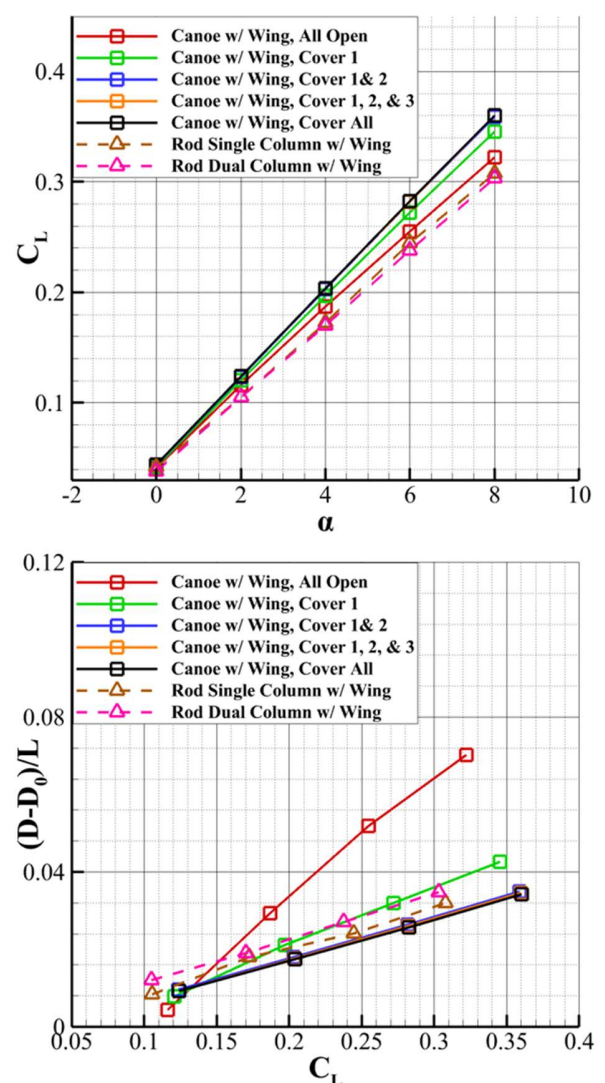
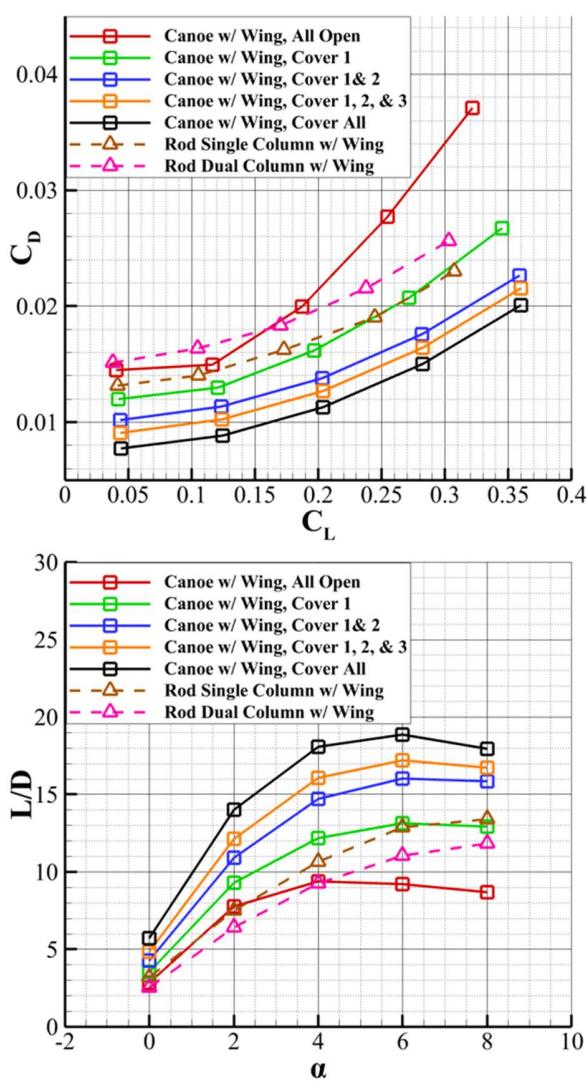


Figure 19 Aerodynamic Properties of Canoe Cases with Wing

EFFECT OF ROTOR PLACEMENTS

The placement of rotors was categorized into two general approaches in the following investigation: placement in spanwise direction and chordwise direction. The spanwise model consists of removing the canoe and placing rotors in a 2×2 distribution, similar to that of the rod case with dual column instead of 1×4 distribution. The chordwise model discussed the relation between aerodynamic properties with respect to rotor distances while holding the canoe size constant.

The two models of interest were shown in Figure 20. The results of the simulation were presented in Figure 21. For comparison purposes, the simulation result of the rod case, previously shown in Figure 11, was also included. Visualization of skin friction coefficient magnitude across the OML is shown in Figure 22. It was observed that an opening on the lifting surface will cause flow recirculation and turbulences that significantly impact the pressure distribution on surfaces after the opening, thus it was preferred to place multiple openings along the chordwise direction to reduce their frontal projection area, i.e., lifting surface area disturbed by openings.

The influence of distance between rotors along the chord of the canoe was then investigated. Considering the center of mass of the entire vehicle, rotor placement was set symmetrical to the center of the canoe, and four different configurations with varying rotor distances with respect to the original canoe configuration were investigated. The distance between rotors was defined by the horizontal distance between two consecutive rotor centers and was nondimensionalized by the diameter of the rotor. For instance, Canoe O-O 2.33 \varnothing indicate that the distance between centers of two consecutive rotors was 2.33 times the diameter of the rotor. A schematic of the geometry of interest was shown in Figure 23. The results of this simulation were plotted in Figure 24. Average differences in drag, as well as geometrical differences, were presented in Table 3.

Not considering the effect of leading edge, rotors placement does not significantly interfere with the aerodynamic properties of the canoe configuration. A pressure coefficient polar of the midspan of the canoe for 2.33 diameter case and 1.77 diameter case were plotted in Figure 24, and it was observed that pressure peaked before and after each opening. This major source of drag existed independent from rotor placement, as the flow will always stagnate at the opening edges facing freestream. However, if the rotors are placed too close together, for instance, the distribution in 1.77 diameter case, the separated flow was not given enough time and space to regain kinetic energy, therefore an increase of drag in that specific case was observed. Furthermore, it was observed that placing openings close to the leading edge causes significant flow separation by reduction in favorable pressure gradient, causing higher gradient of drag coefficient with respect to change in angles of attack.

To conclude this simulation, the relative distance between rotors does not have a significant impact on drag characteristics if the distance between two rotor centers were at least 175% of the diameter of the rotor apart. Placing the first opening away from the leading edge will yield a small amount of reduction in sensitivity of drag with respect to angles of attack as the favorable pressure gradient of the canoe receives less disturbance.

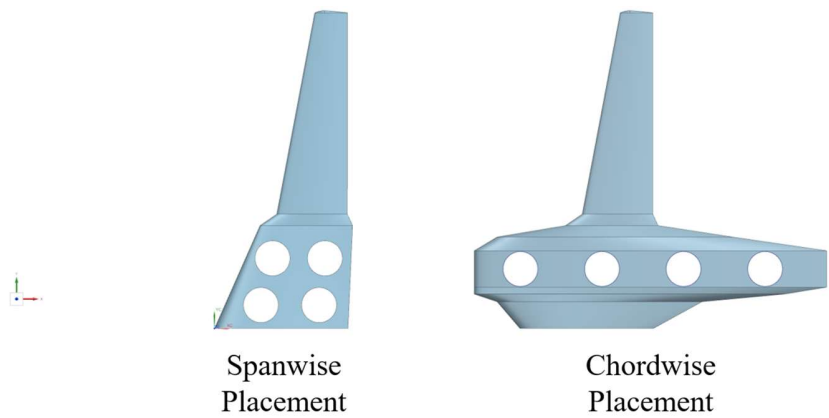


Figure 20 CAD of Canoe Case with Different Rotor Placement Methods

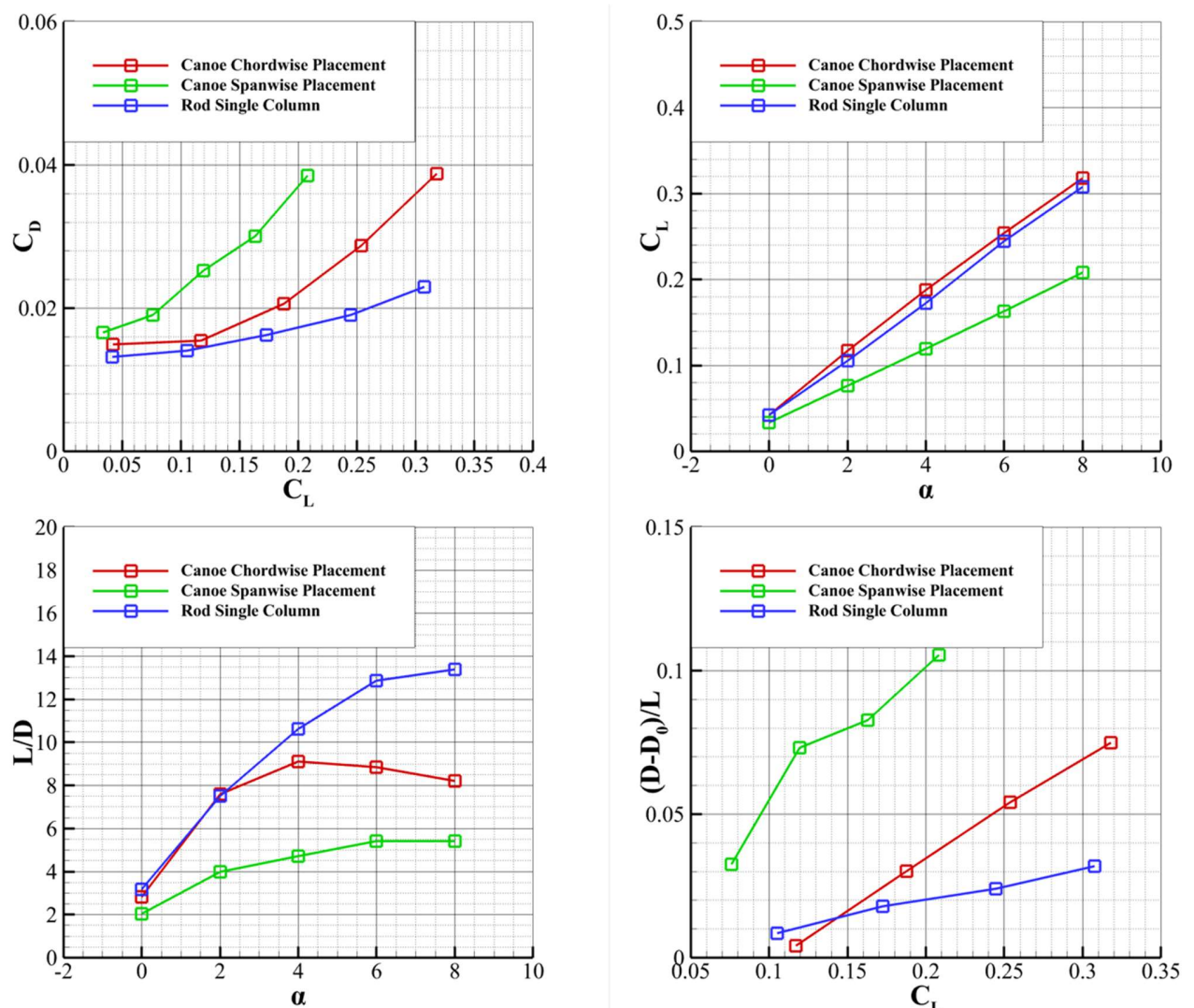


Figure 21 Aerodynamic Properties of Canoe Case with Different Rotor Placements

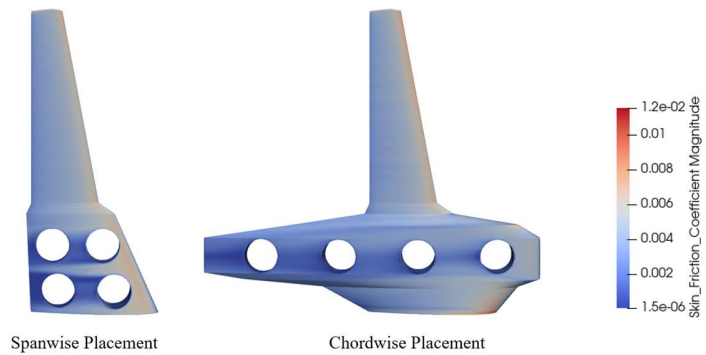


Figure 22 Visualization of Cf Distribution of Canoe Case with Different Rotor Placements

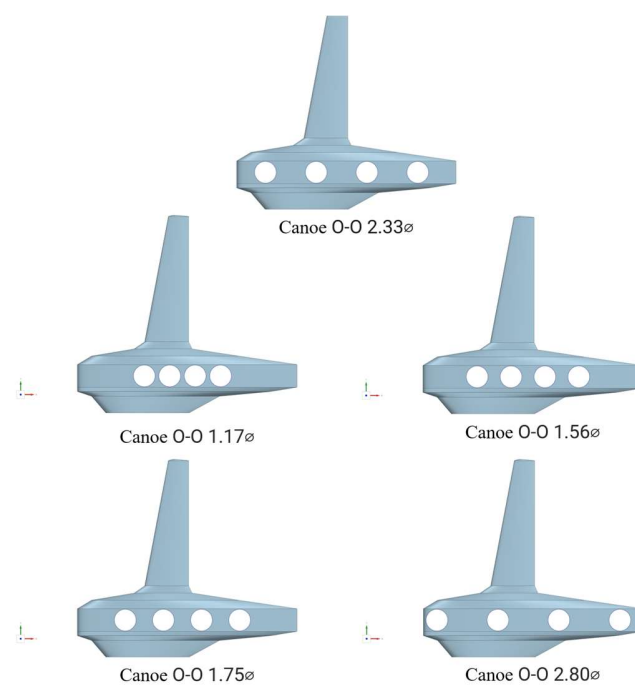


Figure 23 CAD of Canoe Case with Different Rotor Chordwise Distribution

Table 3 Average Drag Difference for Different Rotor Chordwise Distribution

Distance Between Rotor Center (ft)	Distance nondimensionalized by rotor radius	Average Drag Difference (counts)	Average Percent of Drag Difference
4.59	2.33	Baseline	Baseline
2.30	1.17	3.52	1.5%
3.06	1.56	6.64	2.8%
3.44	1.75	7.44	3.1%
5.51	2.80	-14.39	-6.1%

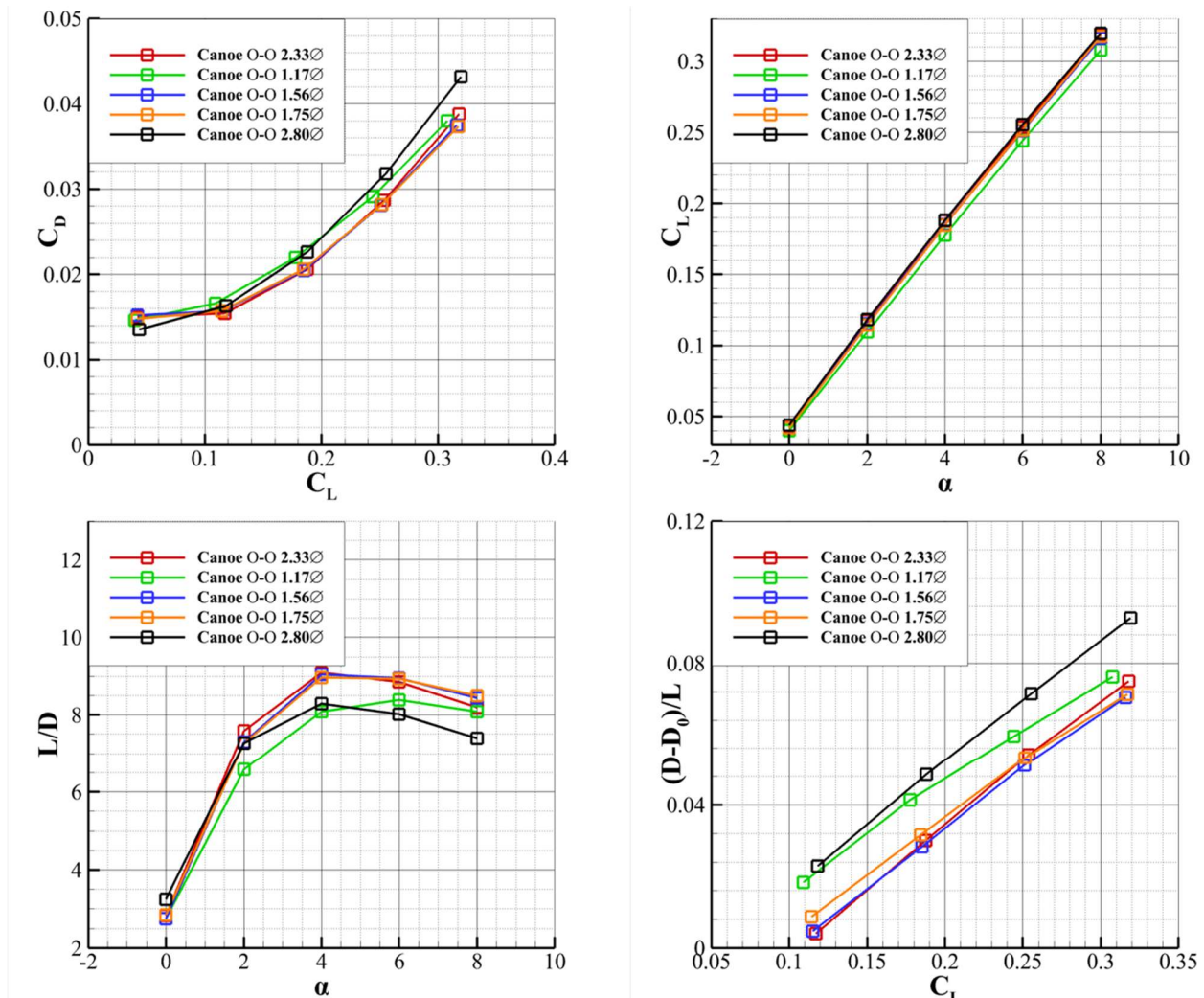


Figure 24 Aerodynamic Properties of Canoe Case with Different Rotor Chordwise Distribution

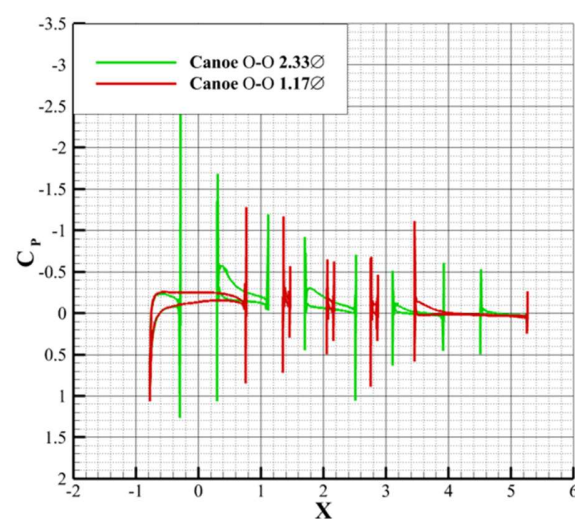


Figure 25 Pressure Comparison of Canoe Section with Different Rotor Chordwise Distribution

EFFECT OF LEADING EDGE MODIFICATIONS

A modification to the investigation above was performed in that the absolute location of the rotors was fixed and the canoe was scaled with respect to the trailing edge in the chordwise direction to allow a greater distance between the first opening and the leading edge. This simulation would offer insight into the absolute location of rotors with respect to the vehicle. Since pressure drag on the canoe decreases as they were put further away from the leading edge, an extended leading edge could suffice the aforementioned goal without clustering rotors. Another consideration was that if rotor doors were to be considered, a smaller curvature of the canoe OML seen by the first rotor would allow easier implementation of such additional elements.

Schematics of geometries considered were shown in Figure 26, where the distance between the leading edge and the edge of the first rotor opening is nondimensionalized by rotor diameter. The result of each simulation was plotted in Figure 27. The simulation can be described as an optimization problem with conflicting objectives: It is desirable that the first opening was placed as far away as possible to the leading edge, but extra surface area will cause more skin friction drag which in turn diminish the drag advantage of a configuration with an overly extended leading edge. When L/D data was plotted for a certain angle of attack, for clarification purposes chosen to be 8 degrees, for all configurations investigated above, as in Figure 28. It was found that the increase follows almost a parabolic increase which slop diminishes as the distance of interest increases.

Another related question was whether the leading edge modification would interfere with the effectiveness of adding the first rotor door. Intuitively, the sensitivity of aerodynamic performance with respect to OML changes, i.e., rotor openings, were higher at the leading edge, thus it was likely that closing the first rotor will not be as beneficial for geometries with longer canoe chord. To address this concern, a set of simulations with varying canoe sizes as described above and a covered first rotor was conducted. The geometries of interest were shown in Figure 29, and the results were presented in Figure 30. For comparison purposes, data from respective cases with all rotors open were also shown in Figure 30. It was observed that once the first rotor was closed, drag reduction caused by increasing canoe chord became trivial, and, unlike observations made in Figure 27, the case with shorter leading edge would slightly outperform the other two cases of interest. It was also observed that reduction of drag caused by closing the first rotor decreases as leading-edge increases. The observations confirmed the explanation offered at the beginning of this paragraph.

Respective drag differences in the above simulations were summarized in Table 4. If no rotor door was added desired distance between the first rotor and leading edge was around 2.8 times the diameter of the rotor opening. This value will be prone to decrease as other driving variables such as weight, stability, and aeroelasticity were taken into consideration. Drag reduction caused by increasing leading edge to first rotor distance was trivial comparing to that caused by covering the first rotor opening, and a longer canoe increases surface friction drag when the rotors were covered. Therefore, adding rotor doors was a more effective choice of decreasing drag compared to increasing canoe chord length.

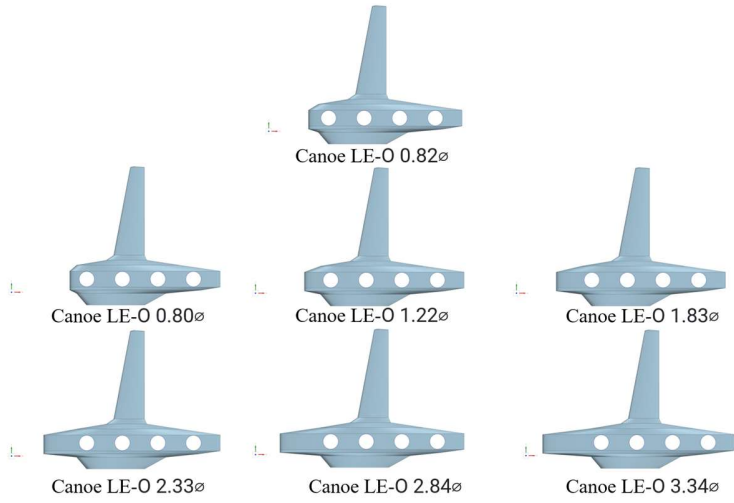


Figure 26 CAD of Canoe Case with Varying Canoe Chord Length

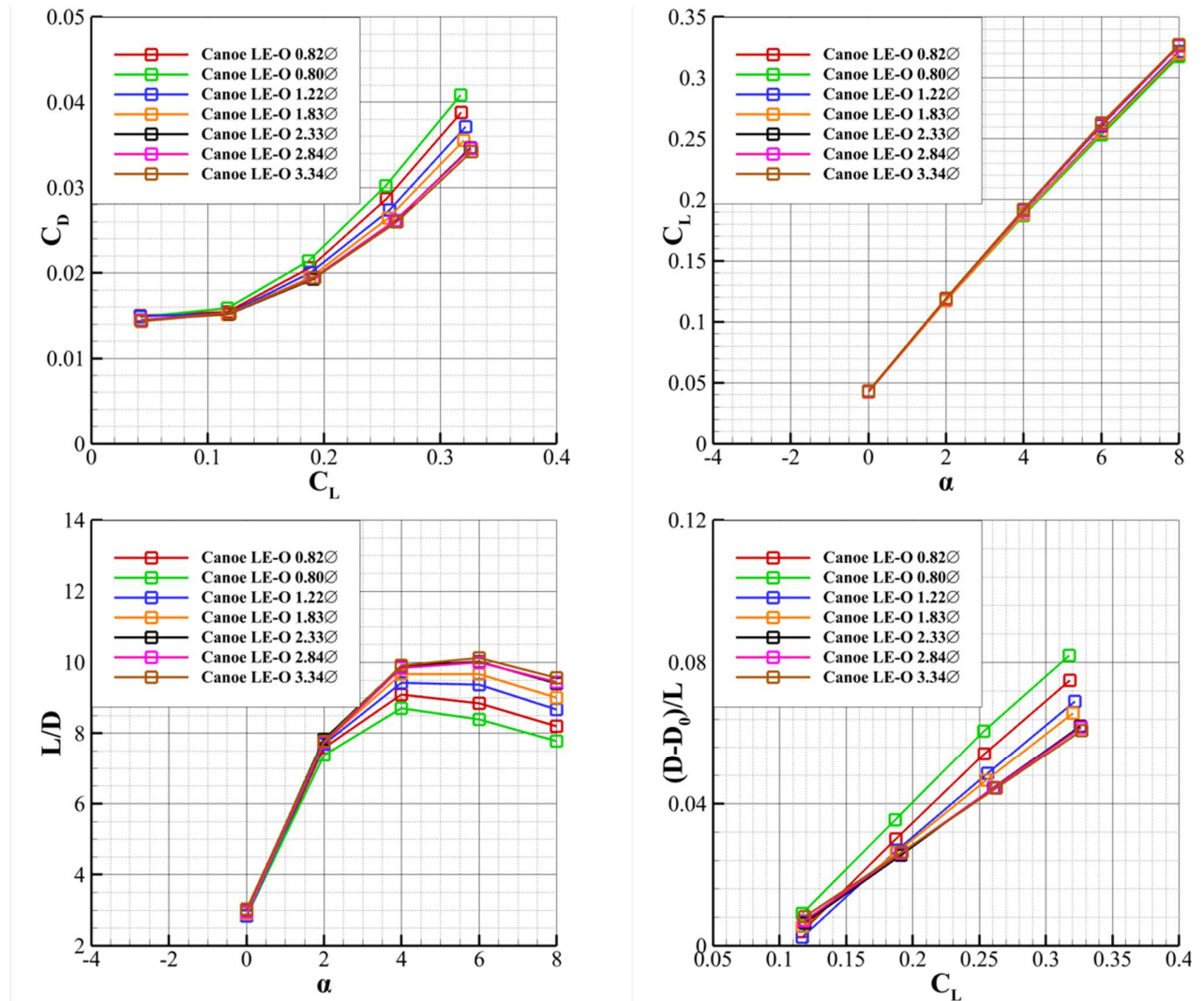


Figure 27 Aerodynamic Properties of Canoe Case with Varying Canoe Chord Length

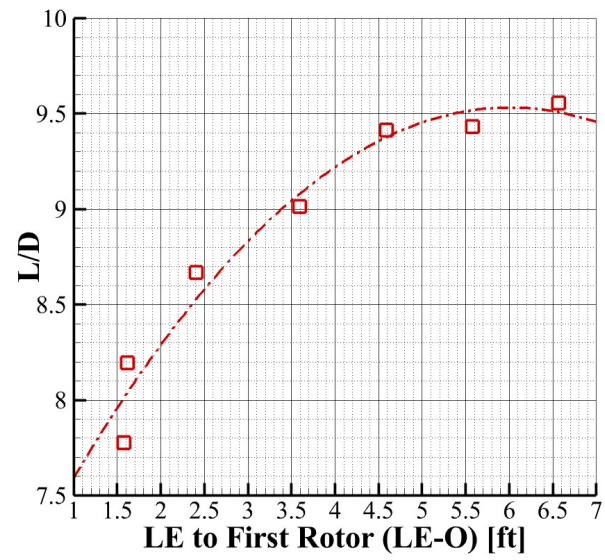


Figure 28 L/D of Canoe Case with Varying Canoe Chord Length at 8 Degree Angle of Attack

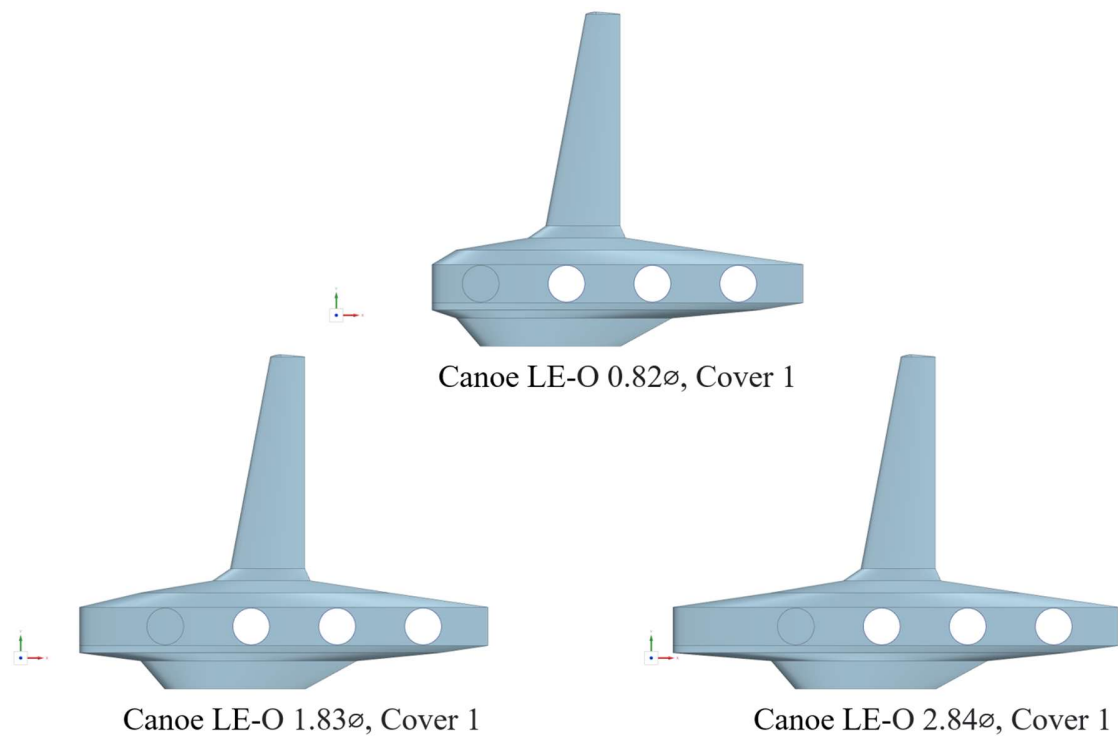


Figure 29 CAD of Canoe Case with Varying Canoe Chord Length with Rotor 1 Covered

Table 4 Average Drag Difference for Varying Canoe Chord Length

Cases	Average Drag Reduction (counts)	Average Percent of Drag Reduction
Canoe LE-O 0.82Ø	Baseline	Baseline
Canoe LE-O 0.80Ø	-9.11	-3.8%
Canoe LE-O 1.22Ø	7.89	3.3%
Canoe LE-O 1.83Ø	15.06	6.4%
Canoe LE-O 2.33Ø	17.81	7.5%
Canoe LE-O 2.84Ø	17.34	7.3%
Canoe LE-O 3.34Ø	18.69	7.9%
Canoe LE-O 0.82Ø, Cover 1	60.00	25.3%
Canoe LE-O 1.83Ø, Cover 1	56.00	23.6%
Canoe LE-O 2.84Ø, Cover 1	51.38	21.7%

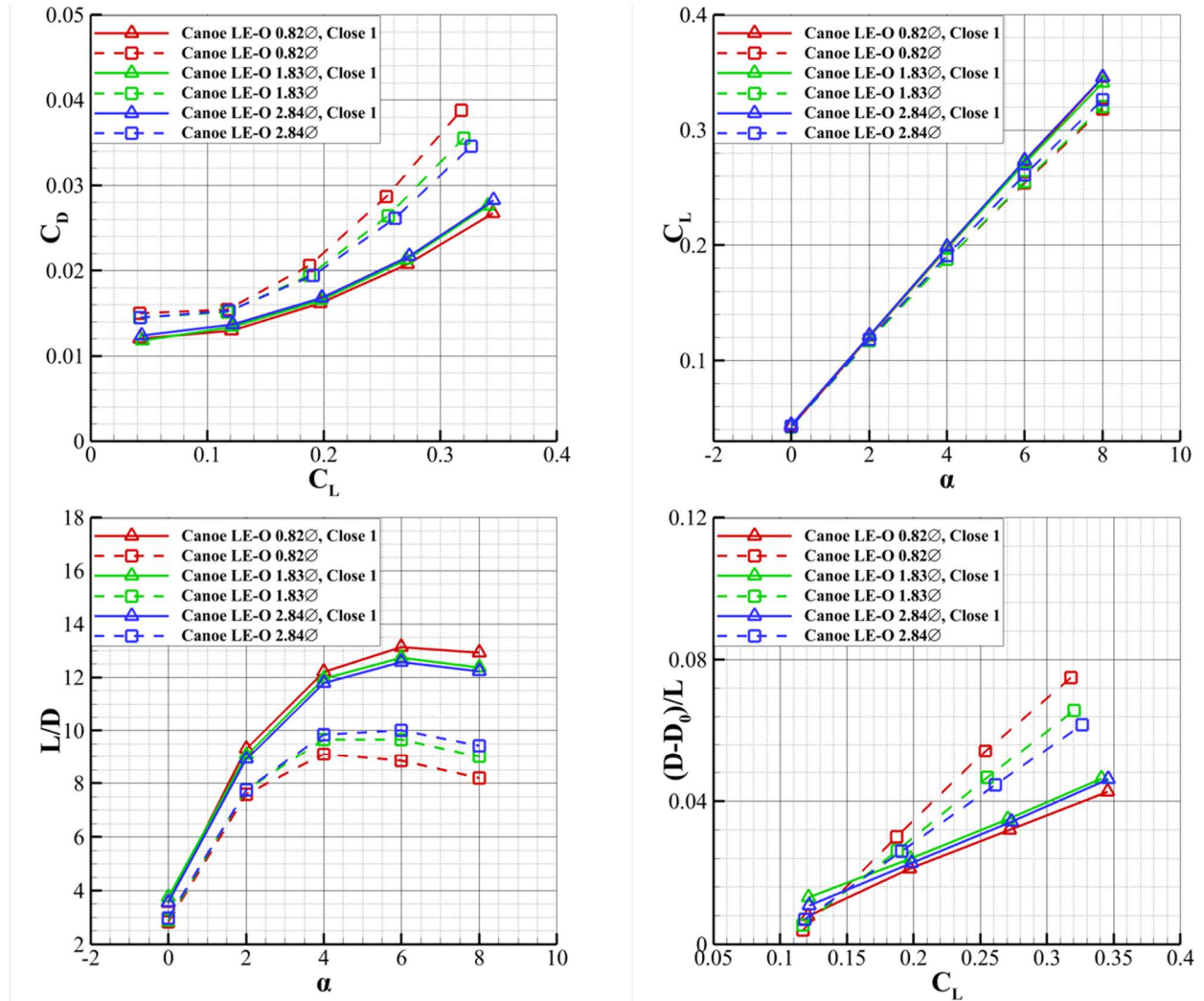


Figure 30 Aerodynamic Properties of Canoe Case with Varying Chord Length, Rotor 1 Covered

EFFECT OF ROUNDING ROTOR EDGES

A rounded rotor edge would facilitate better propulsive efficiency of lifting fans by increasing intake area and thus vertical mass flow rate. Furthermore, a rounded edge might allow the stagnate flow to be better attached to the surface OML and thus reducing turbulences caused by separation. A configuration with rounded rotor openings at the suction surface was made by expanding rotor diameters by half on the canoe surface. A C_p distribution along the geometry of interest was shown in Figure 31, and C_p distribution along the midspan slice of the canoe was presented in Figure 32. It was observed that the aforementioned approach did not eliminate flow stagnation but diffused the turbulence observed on rotor edges. A comparison of aerodynamic coefficients was made with the canoe case with straight rotor edge, shown in Figure 33. Rounding rotor edges helped in decreasing the sensitivity of drag to an increase in angles of attack and acquired slightly better aerodynamic performances in cases with higher angles of attack. This was contributed by less turbulence induced

by the smooth continuous OML compared to the almost vertically placed straight edges. However, the rounded rotor edges also increased surface area and thus would experience more drag at low angles of attack. A trade study with driving factors including weight, aerodynamic performances, and lifting fan efficiency would have to be conducted to determine whether rounding rotor edges was necessary.

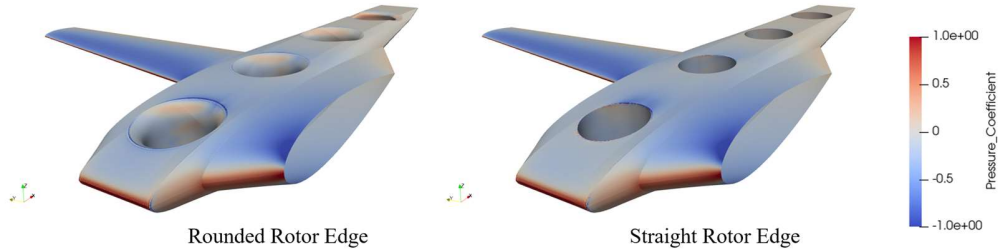


Figure 31 Cp distribution of Canoe Case with Rounded Rotor Edge

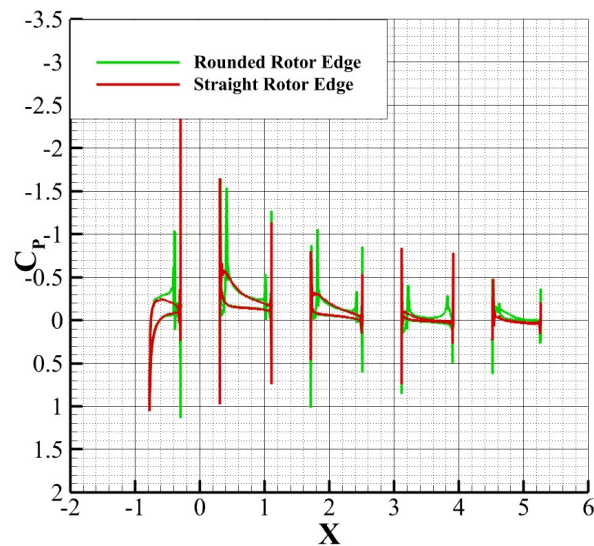


Figure 32 Pressure Comparison of Canoe Section with Rounded Rotor Edge

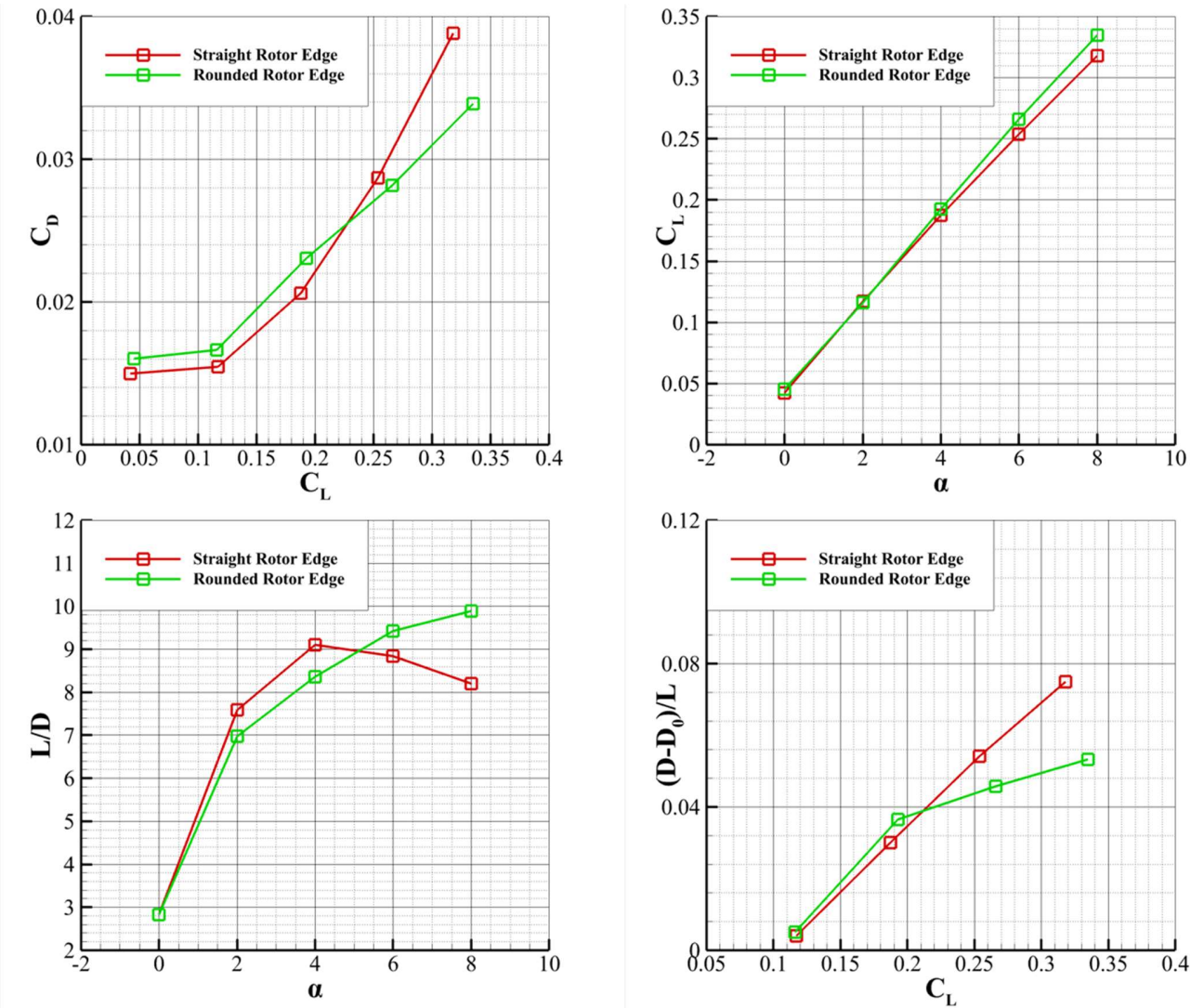


Figure 33 Aerodynamic Properties of Canoe Case with Rounded Rotor Edge

EFFECT OF ROTOR DIAMETERS

The rotor diameter for the current study was set to be 1.96 ft, and a larger opening would decrease the aerodynamic performance of the current configuration. However, the major driving variable for rotor diameter was not aerodynamic efficiency but propulsive performance at vertical lift off. Four variations of the baseline configuration with variable rotor diameter while holding all other aspects constant were made, outlined in Figure 34, and simulated. The results of this simulation were plotted in Figure 35. For comparison purposes, results of canoe with all rotors covered were included as an extreme case with rotor diameter equals to zero. It was observed that the relation between aerodynamic properties and diameter, as well as angles of attack, follows parabolic relationships. To better visualize the data and draw a correlation, a contour plot is made for L/D versus Angles of attack and diameter of rotor openings, in ft, plotted in Figure 36.

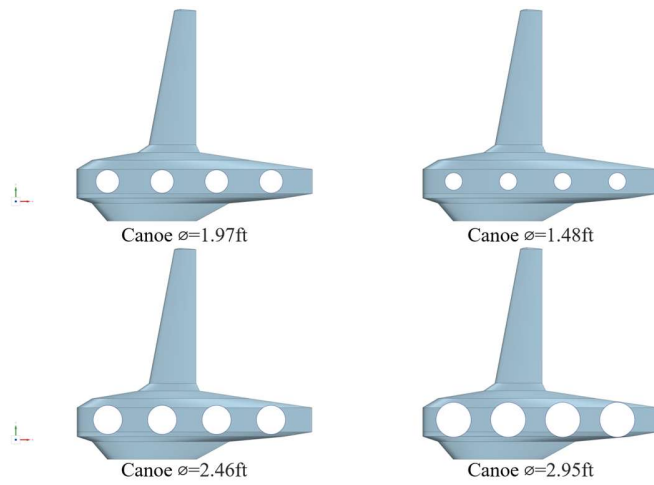


Figure 34 CAD of Canoe Case with Different Rotor Diameter

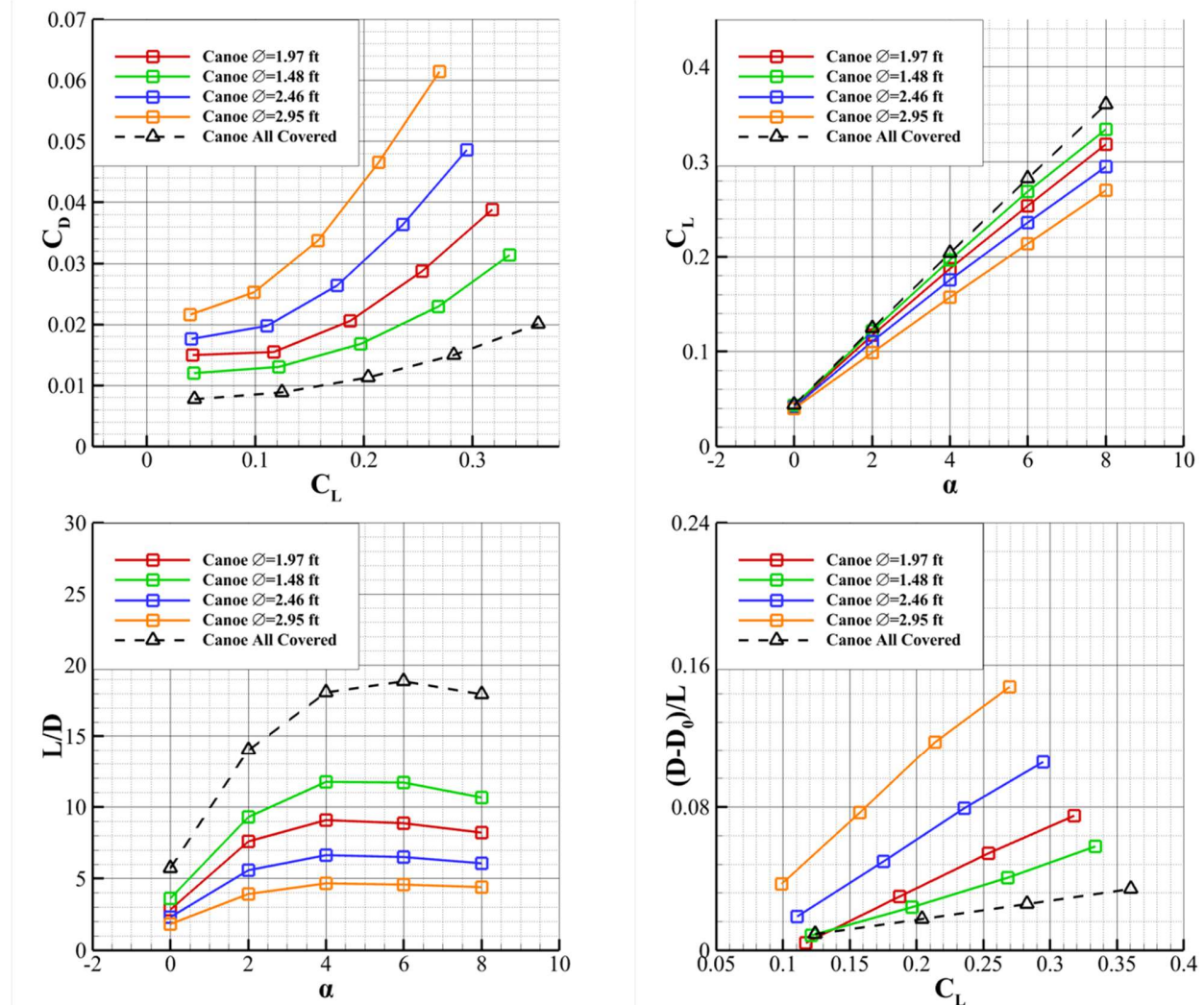


Figure 35 Aerodynamic Properties of Canoe Case with Different Rotor Diameter

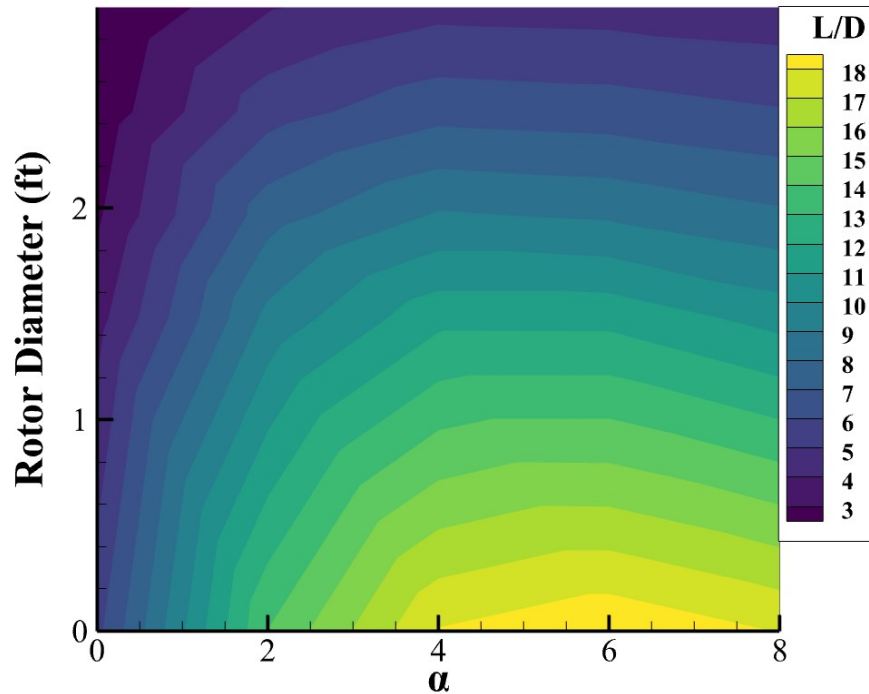


Figure 36 L/D Contour of Canoe Case with Different Rotor Diameter

CHAPTER 5: FULL CONFIGURATION SURVEY

Simulation for entire configurations, with both open and shrouded rotors, were conducted to ensure that the pros and cons of different rotor installment methods were still significant when other components such as fuselage and tails were taken into consideration. The three models of interest were presented in Figure 37. Results from the simulation were presented and compared in Figure 38. Comparing results presented in Figure 11, it was observed that while fuselage and tail brought a significant amount, on average 180 counts, of drag, advantages of the canoe over rod configuration were still evident. The drag built up of fuselage and tail superpose almost linearly to aerodynamic characteristics of the wing for the canoe and the rod case respectively.

It was also observed that the wing-fuselage junction for the rod case caused less induced drag than the canoe case, as visualized by the C_p distribution illustrated in Figure 39. This was mainly due to the lack of the inversely tapered junction between the canoe and the fuselage. This would become more significant if the leading edge is extended compared to the baseline configuration as discussed in Chapter 4. Possible solutions to address this concern were to extend the fuselage and remove the junction between canoe and fuselage, by which moving the entire wing section inboard or decrease canoe chord length and add rotor doors to the first two openings.

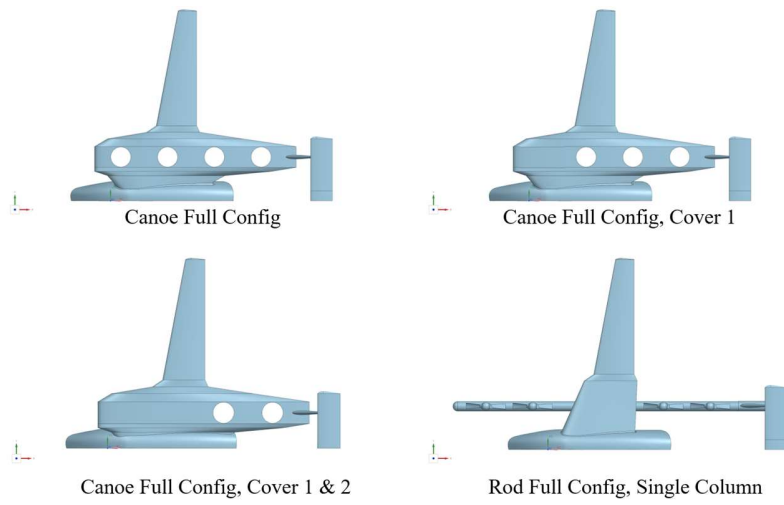


Figure 37 CAD of Canoe and Rod Cases with Fuselage and Tail

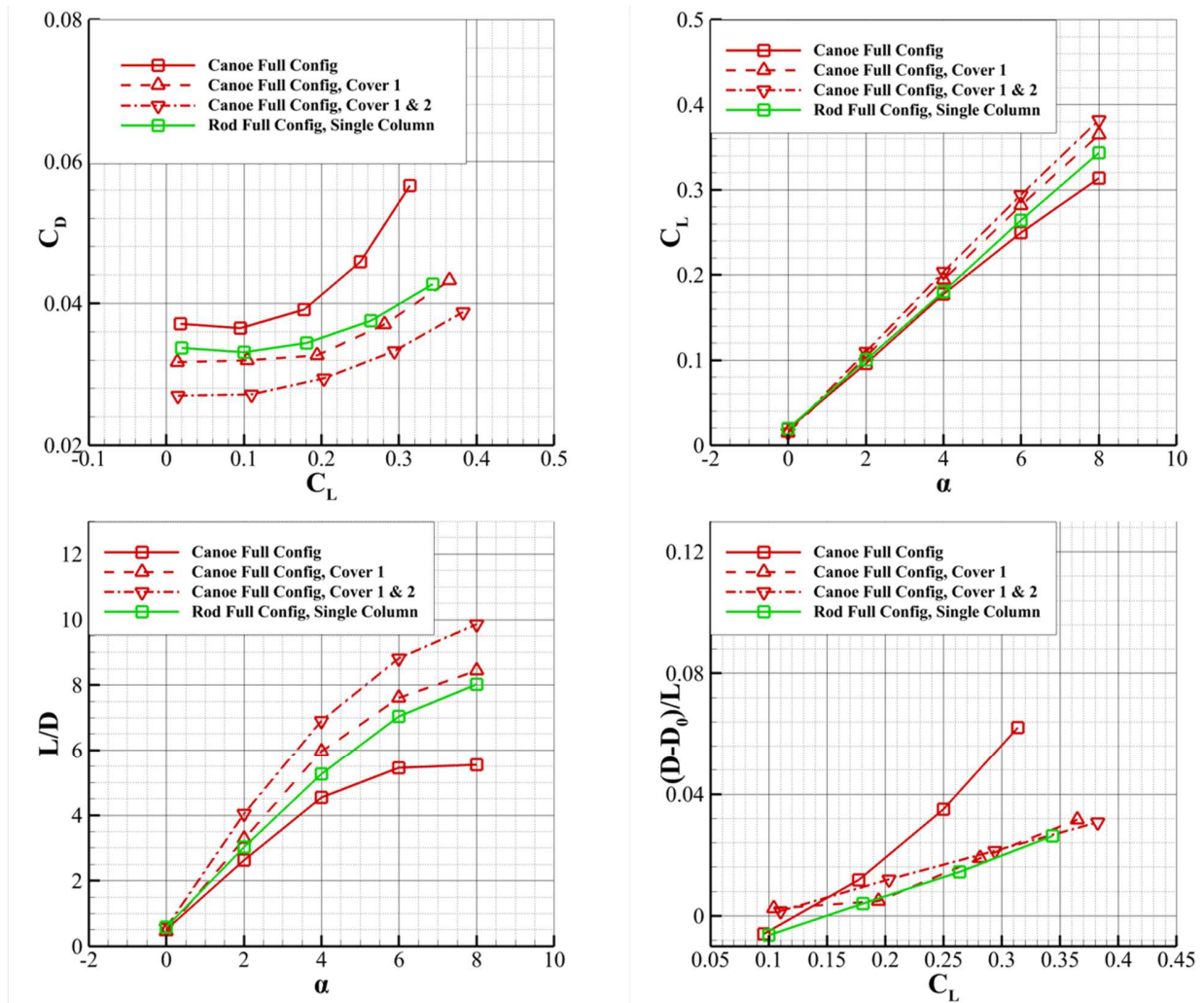


Figure 38 Aerodynamic Properties of Full Configurations

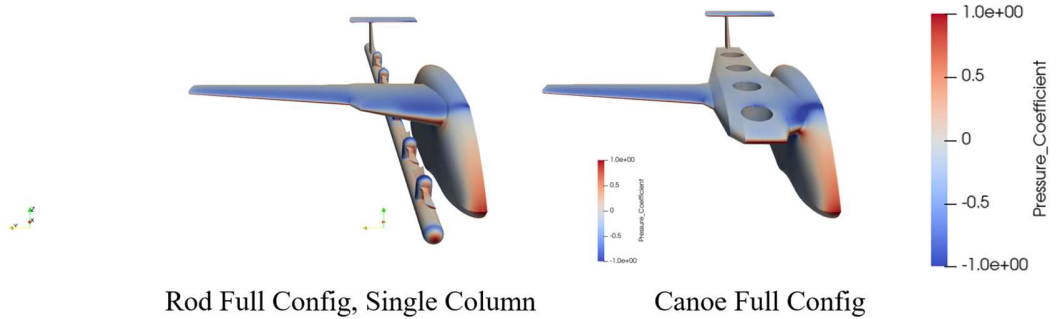


Figure 39 Cp Distribution of Full Configuration

CHAPTER 6: CONCLUSION AND FUTURE WORK

This study investigated aerodynamic properties of different eVTOL designs, as well as potential modifications of the canoe configuration. Modifications and driving factors considered in this study included rotor doors, re-arranging rotor placement, canoe sizing, and rotor diameters were discussed and results were concluded individually as follows. A summary of all configurations investigated above was summarized in Table 5. The angle of attack of 2 degrees was chosen to be a representative flight condition in Table 5, and the order of trade elements followed that presented in this report. Trade elements that have significant impacts in drag were highlighted using asterisk marks.

Varying canoe thickness does not significantly change drag characteristics. As decreasing canoe thickness by 25%, with last two rotors open increased drag coefficient by 5 counts and decreasing canoe thickness by 25% with all rotors sealed decreased drag coefficient by 10 counts. This slight variation was small compared to advantages brought by changing leading edge length or adding canoe doors.

Rotor doors will significantly improve the drag characteristics of the canoe case. Both upper and lower surfaces of a rotor opening need to be closed to receive optimal results, and closing the first three rotor openings can receive on average 38%, or 100 counts, of drag coefficient reduction. Among all rotor doors, closing the ones closest to the leading edge have a better effect in reducing drag than closing that near the trailing edge, and covering the first rotor will cause similar drag coefficients to that of rod single column case.

Rotors should be placed vertically in the chordwise direction to reduce their frontal projection area. The separated flow was observed after each rotor opening, thus placing rotors in the spanwise direction will impact the effectiveness of the wing. Placing rotors closer together does not significantly influence the aerodynamic performance of the geometry, but placing the first opening closer to the leading edge would result in early separation caused by decreased favorable pressure gradient regime. If no rotor doors were added, the first opening should be placed 2.8 times the rotor diameter away from the leading edge for drag reduction. If rotor doors were added, drag reduction

caused by leading edge modification was small, and the distance between leading edge to the first rotor can be left as small as possible.

Significant stagnation was observed at the opening edges facing directly toward or against the freestream. This was identified as a major source of pressure drag to the current configuration. Rounding rotor openings did not impact drag experienced but could be added to facilitate vertical mass flow rate when running lifting fans.

The effect of rotor diameter on drag characteristics of the canoe configuration was shown to follow a parabolic relationship. Larger opening diameters will increase drag received by the canoe, but it was important to note that the main driver of rotor diameter was propulsive efficiency at liftoff rather than aerodynamic efficiency at cruise.

Table 5 Summary of Trade Elements and Respective Drag Differences

Trade Element	Baseline	New	Baseline CD at AoA 2 (counts)	New CD at AoA 2 (counts)
Rod/ Canoe with Wing *	Canoe	Rod Single Column	154.47	140.29
Canoe Thickness	1.2 ft	0.9 ft	113.25	113.42
Canoe Door *	All Open	Cover 1	154.47	129.48
Canoe Door *	All Open	All Covered	154.47	88.62
Canoe Rotor *	Single Column	Dual Column	154.47	190.38
Canoe Rotor Spacing	O-O 2.33 \varnothing	O-O 1.56 \varnothing	154.47	157.51
Leading Edge *	LE-O 1.22 \varnothing	LE-O 2.84 \varnothing	154.47	118.47
Leading Edge	LE-O 1.22 \varnothing	LE-O 0.80 \varnothing	154.47	158.61
Leading Edge	LE-O 1.22 \varnothing , 1 Covered	LE-O 2.84 \varnothing , 1 Covered	129.48	136.61
Round Rotor Edge *	Straight	Rounded	154.47	166.24
Rotor Diameter	$\varnothing=1.97\text{ft}$	$\varnothing =1.48\text{ft}$	154.47	130.47
Rotor Diameter *	$\varnothing=1.97\text{ft}$	$\varnothing=2.95\text{ft}$	154.47	252.51
Full Configuration *	Canoe, All Open	Rod Single Column	365.00	330.69
Full Configuration *	Canoe, All Open	Canoe Cover 1	365.00	319.32

* Elements that results in significant aerodynamic property changes

When the configurations are simulated with other components such as tail and fuselage, the improvements and advantages mentioned above were still significant. Flow separation was observed at the inboard edge of the canoe, and the wing-fuselage junction of the canoe case received more drag than that of the rod case.

Future studies should be based on a new configuration integrating all suggestions mentioned above. A first representation of the next design iteration was shown in Figure 40. The new configuration, compared to the ones discussed in this report, will improve upon the canoe case with shorter canoe, first two rotors covered by rotor doors, more compact rotor spacing, rounded rotor edges, and better wing-fuselage junction. Future studies should also discuss different shapes of fuselage and their aerodynamic properties. For the current study, the fuselage was only initially examined and large separation was observed behind the vertical end of the fuselage. Stability of this vehicle should also be taken into consideration in the future, as the suggested shortening of canoe may interfere with control efficiency of tail. Finally, an MDO problem could be performed on the wing-canoe section for better performance. The problem would consider weight, aeroelasticity, and aerodynamics as objectives, and optimize the wing OML to better fit the mission profile.

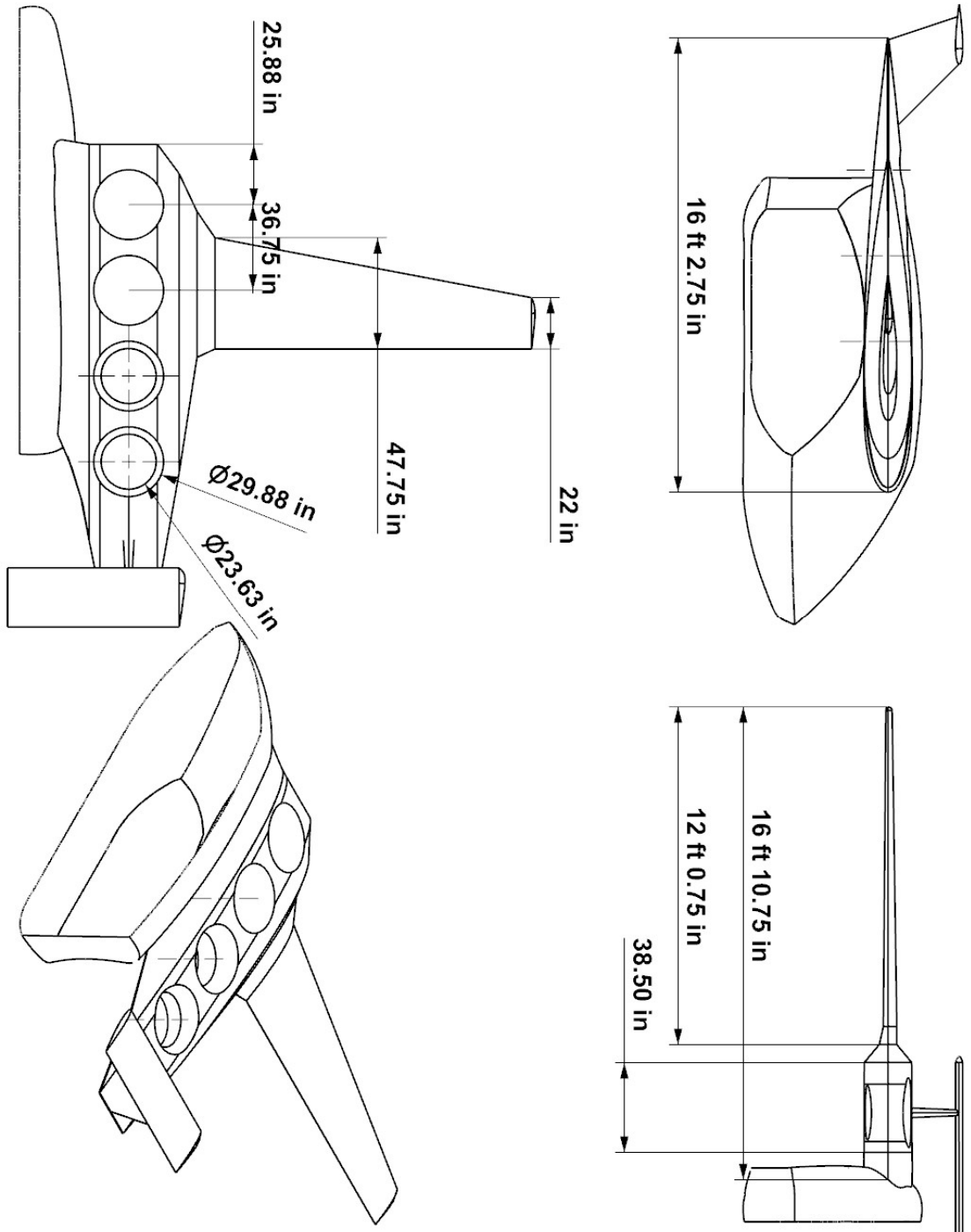


Figure 40 CAD of Possible New Configuration

REFERENCES

- [1] Ng,W., Patil, M., and Datta, A., "Hydrogen Fuel Cell and Battery Hybrid Architecture for Range Extension of Electric VTOL (eVTOL) Aircraft", *Journal of the American Helicopter Society*, Vol.66(1), 2021, pp. 1-13. <https://doi.org/10.4050/jahs.66.012009>.
- [2] Moore, M., "NASA Puffin Electric Tailsitter VTOL Concept", 10th AIAA Aviation Technology, Integration, and Operations (ATIO) Conference, 2010, pp.13-15, American Institute of Aeronautics and Astronautics, doi:10.2514/6.2010-9345.
- [3] AHS international leads Transformative Vertical Flight Initiative. News on electric vertical takeoff & landing (eVTOL) aircraft, <https://evtol.news/news/ahs-international-leads-transformative-vertical-flight-initiative>.
- [4] "Pioneering the Urban Air Taxi Revolution," Volocopter, 6 June 2019. [retrieved 22 March 2022].
- [5] Home Page, Tier 1 Engineering, <https://www.tier1engineering.com/>, [retrieved 22 March 2022].
- [6] Urban Air Mobility, Volocopter, <https://www.volocopter.com/urban-air-mobility/>, [retrieved 22 March 2022]
- [7] Pipistrel unveils 801 Evtol at Uber's Elevate Summit, Pipistrel Aircraft, <https://www.pipistrel-aircraft.com/pipistrel-unveils-801-evtol-at-ubers-elevate-summit-archive/>, [retrieved 22 March 2022]
- [8] Joby Aviation, Joby, <https://www.jobyaviation.com/>, [retrieved 22 March 2022]
- [9] Lilium jet - the first electric VTOL (EVTOL) jet, Lilium, <https://lilium.com/jet>, [retrieved 22 March 2022]
- [10] Evtol classifications, News on electric vertical takeoff & landing (eVTOL) aircraft, <https://evtol.news/classifications/>, [retrieved 22 March 2022]
- [11] Hascaryo R. W., and Merret J.M., "Configuration-Independent Initial Sizing Method for UAM/eVTOL Vehicles", AIAA Aviation 2020 Forum, <https://doi.org/10.2514/6.2020-2630>
- [12] Economou, T. D., Palacios, F., Copeland, S. R., Lukaczyk, T. W., and Alonso, J. J., "SU2: An Open-Source Suite for Multiphysics Simulation and Design," *AIAA Journal*, Vol. 54, No. 3, 2016, pp. 828-846. <https://doi.org/10.2514/1.J053813>
- [13] Mesh generation software for CFD: Pointwise, Inc.. Mesh Generation Software for CFD | Pointwise, Inc, <http://www.pointwise.com/>, [retrieved 22 March 2022]